Evaluation of Vegetation Effects on the Generation and Modification of Mesoscale Circulations

M. SEGAL AND R. AVISSAR

Department of Atmospheric Science, Colorado State University, Fort Collins, Colorado

M. C. MCCUMBER

Laboratory for Atmospheres, NASA/Goddard Space Flight Center, Greenbelt, Maryland

R. A. PIELKE

Department of Atmospheric Science, Colorado State University, Fort Collins, Colorado

(Manuscript received 29 May 1987, in final form 1 February 1988)

ABSTRACT

The purpose of the present study is to evaluate (i) the effect of vegetated surfaces on modifying sea breeze and daytime thermally induced upslope flows; and (ii) the generation of thermally induced flow by vegetated areas contrasted by bare soil areas. In order to address these objectives, the following tasks were carried out: 1) previous documented studies with implication for (i) and (ii) are reviewed; 2) the main features of the thermal balance of vegetated surfaces are outlined qualitatively; 3) a quantitative evaluation of the various components in the thermal balance based on documented observational studies is provided; and 4) scale analyses and numerical model simulations are used to provide quantitative evaluations of the circulations involved with (i) and (ii) for several illustrative cases.

The study suggests that the impact of vegetated surfaces in those cases is highly dependent on the environmental conditions as well as vegetation characteristics. For ideal environmental conditions resulting in high evapotranspiration rates over extended dense vegetated areas, it is shown that the circulation types listed in (i) are substantially reduced. For the situation described by (ii), circulations with an intensity close to that of a sea breeze can develop when the vegetation is very dense, and covers an extended area, and under favorable environmental conditions. The reduction in these impacts for more frequent real world situations involved with less favorable environmental conditions as well as with relatively sparse vegetated areas is also evaluated.

1. Introduction

The presence of vegetation is expected to modify the surface thermal fluxes as compared to those of an equivalent bare soil surface under the same environmental conditions. Consequently, the partitioning of thermal energy between sensible and latent heat fluxes (i.e., the Bowen ratio) is likely to be different for both surfaces. Documentation in the research literature provides a variety of observational and modeling evaluations of this thermal flux partitioning. Common daytime mesoscale circulations such as sea breezes or thermally induced upslope flows are directly related, in their intensities, to the magnitude and the horizontal distribution of the surface sensible heat fluxes. Therefore, the characteristics of these circulations are likely to be modified in the presence of vegetation (as compared to bare soil conditions). Extensive vegetated areas adjacent to water bodies or in locally elevated terrain are common in many subtropical and midlatitude geographical locations. Vegetated areas adjacent to dry bare soil regions (as common, for example, in regions of summer agricultural land use) may provide substantial gradients of sensible heating which result in the onset of thermally induced mesoscale circulations. The alteration of existing mesoscale circulations or the generation of mesoscale systems as suggested above may be of importance in weather prediction and environmental assessments. Several observational studies hypothesized that such mesoscale features may be involved with triggering and development of convective clouds (e.g., Hammer 1970; Burman et al. 1977; Barnston and Schickedanz 1984; Wilson and Schreiber 1986).

It is anticipated that the strongest forcing of thermal circulations by a vegetated area is involved with large irrigated vegetative areas in semiarid or relatively dry locations. Geographical areas in the United States in which large vegetated areas are contrasted by such sur-

Corresponding author address: Moti Segal, Dept. of Atmospheric Sciences, Colorado State University, Fort Collins, CO 80523.

roundings include, for example, the San Joaquin and Sacramento Valleys, and the area adjacent to the Salton Sea in California; the eastern plains of Washington State; and the Snake River area in Idaho. Along the Nile River in Egypt and the Sudan, vegetated areas reach in some locations 30 to 40 km in width, with an even larger extent at the Nile Delta where the river empties into the Mediterranean Sea. The Lake Chad basin in Africa becomes vegetated during the fall months, generating surface IR temperature contrasts reaching 14°C between the vegetated area and the surrounding desert (Schneider et al. 1985). The irrigated areas of Mesopotamia and the Indus River basin in Pakistan, some irrigated regions in the Soviet Union (see for example Dzerdzeevskii 1963), as well as the extended irrigated areas along the Murray and Murrumbidgee Rivers in southeastern Australia provide additional examples of mesoscale domains with a potential sharp thermal contrast. In the era of increasing satellite imagery resolution, identification of smaller areas involved with such a contrast, and evaluation of the surface thermal contrast, is likely to be a straightforward task.

Evaluation of the characteristics of the thermal circulations in the aforementioned situations is in its infancy. It is the purpose of the present study to provide a systematic evaluation of the effect of vegetation cover on the possible generation or modification of mesoscale circulations. The nature of the evaluation first requires an overview of existing relevant studies (section 2). Evaluation of various aspects relating to the thermal forcing of these circulations as affected by vegetation and soil properties are given in section 3. This investigation includes tabular and graphical illustrations which are related to scale analysis (section 4) and to numerical model evaluations (sections 5 and 6). Finally it is worth noting, the present study considers a specific case of nonclassical mesoscale circulations (NCMC) forced by differential surface heating. NCMCs are anticipated to develop because of surface horizontal heterogeneity, for example, in soil wetness, in cloud shading, or in snow cover (see Segal et al. 1984 and Pielke and Segal 1986 for general evaluations of NCMC). Some results obtained in previous NCMC studies are adopted in this study for comparisons.

2. Overview of previous pertinent studies

This overview focuses on aspects related to flat terrain induced circulations. Apparently, no observational or modeling efforts have been involved with the influence of vegetation cover along slopes, on the related daytime thermally induced flows.

a. Modeling evaluations

Relatively little attention has been given in the research literature to a modeling evaluation of the influence of vegetation cover on mesoscale circulations. An interactive atmospheric–vegetation–soil model was applied by McCumber (1980), who evaluated, among other aspects, the effect of the vegetation on the development of the summer sea breeze over South Florida. That study also indicated possibly significant induced mesoscale circulations involved with sharp horizontal changes in the character and type of the vegetation cover. Garrett (1982) included a vegetation module in his model while studying the interactions between convective clouds, the convective boundary layer, and forested surfaces. Yamada (1982) incorporated vegetation in a planetary boundary-layer model while studying air circulations in the lower atmosphere.

In the aforementioned studies, however, no attempt was made to explore quantitatively and systematically the impact of vegetation on the generation and modification of mesoscale systems. Probably the first attempt to evaluate expected circulations between a vegetated area contrasted by bare soil is reported by Anthes (1984). That study provides an evaluation of the anticipated thermal contrast in subtropical latitudes. In addition it provides scaling by means of a linear analytical model, illustrating the possible characteristics of mesoscale circulations involved with such contrasts.

b. Near-surface temperature observations

Most of the observational studies devoted to evaluating the effect of vegetation cover (mostly those involved with irrigated crop areas) on meteorological shelter temperature, as contrasted by bare soil situations under the same environmental conditions, indicate noticeable air temperature differences. It is suggested that most of the drop in temperature over irrigated crop areas are due to evapotranspiration contributed by crop transpiration and the wet soil evaporation. It is worth noting, however, that the evaporation of water during irrigation itself is another factor contributing to this drop (e.g., Lomas and Mandel 1973; Budyko 1977, p. 174). De Vries and Birch (1961) reported an average decrease in air temperature of 1°–2°C (at a height of 1.25 m) in the middle of an irrigated area as compared with observations at a dry-land station 8 km away. Davenport and Hudson (1967) studied the variations of the air temperature along a 17 km transect which included an irrigated area within the arid region of Sudan Gezira. They found that the irrigated area (at 2 m height) had a daily mean temperature that was approximately 1.5°C lower than the surrounding dry area. In a similar type of temperature measurement, during the summer in Kimberly, Idaho, Burman et al. (1975) found the daytime temperature to be 3.1°C cooler over the irrigated area (see Fig. 1a). Similar features of air–temperature depression over small irrigated areas in the desert of southern Israel are reported in Sebba et al. (1984). Barnston and Schickedanz (1984) studied the development of "islands" of irrigated areas in the western Great Plains of the United States during the

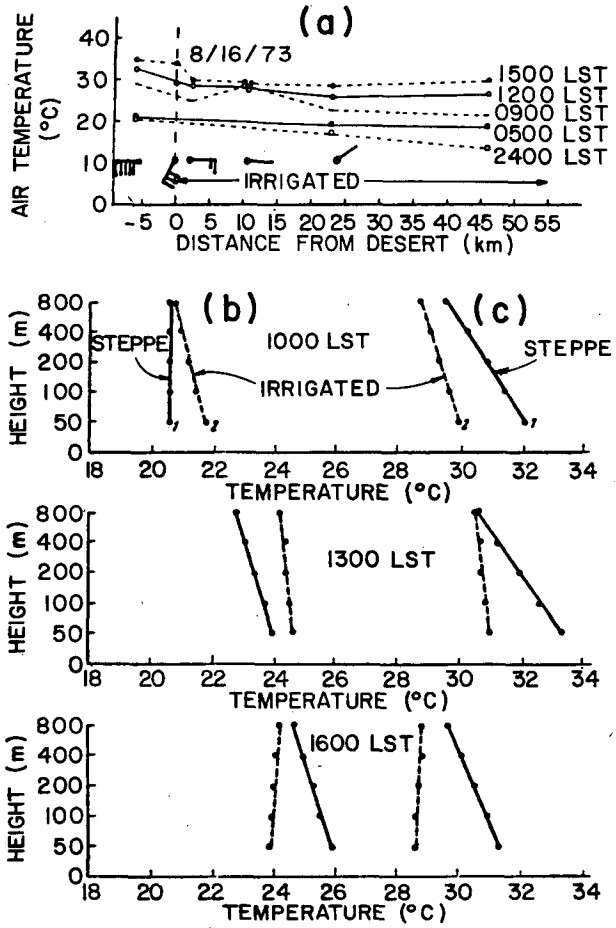

FIG. 1. (a) Transect through desert and irrigated areas in the vicinity of Kimberly, Idaho providing surface air temperature and surface wind (each barb indicates a wind speed increment of 1 m s^{-1}) on 08/16/73 (adopted from Burman et al. 1975); (b) Observed vertical distribution of the temperature in an irrigated area as contrasted to an adjacent steppe after a heavy rain the previous night and (c) During dry weather conditions (adopted from Dzerdzeevskii 1963).

years 1939–69. Focusing on the eastern Texas Panhandle, they found that irrigation appears to lower the daily maximum summer air temperature by about 2°C during synoptically undisturbed periods. In a relatively small irrigated area in the Trans-Volga steppe in the Soviet Union, Dzerdzeevskii (1963) observed an average temperature difference of about 4.5°C during the summer. This study will show that such observed contrasts of air temperature are capable of generating noticeable mesoscale thermal circulations.

c. *Boundary-layer thermal contrast*

Very little documentation is available as to the depth to which the horizontal temperature gradient extends. Holmes (1970) measured a noticeable thermal gradient within the lower 60 m over varied agricultural land near Brooks, Alberta. Under light synoptic winds, the temperature difference, at 20 m height, between the irrigated area and the adjacent prairie reached 4°C. Dzerdzeevskii (1963) provided observed vertical distributions of temperatures above irrigated areas as contrasted to the related temperatures above an adjacent steppe after heavy rain the previous night (Fig. 1b) and during dry weather conditions (Fig. 1c). The thermal difference in the dry case is noticeable to a height of about 1 km. Following the rain event the thermal contrast was reversed in the first half of the day, while reestablished somewhat in the afternoon hours. In the cotton area of Pakhta–Aral, which is situated on 100 km^2 of irrigated land in the arid area of South Kazakhstan, Vo ronstov (1963) observed that the average temperature difference in July was 4°C in the lowest 50 m decreasing to 1°–1.5°C at 400 m. At 700 m the temperature over the irrigated area and the surrounding arid zones were virtually equal. During the CINDE (Convective Initiation and Downdraft Experiment) project in summer 1987, aircraft measurements were carried out in the lower atmosphere along contrasts of irrigated dryland area in northeast Colorado (see Fig. 11a for surface temperature contents in this area). The data which is currently being processed indicates very noticeable thermal and moisture gradients across these two areas.

d. *Flow features*

Direct evidence of the existence of thermally induced circulations between vegetated areas and an adjacent bare soil domain could be provided if the mesoscale and local flow were adequately observed. Unfortunately the observations required to identify such flow features are, in general, not documented in the literature, nor are they available as archived data. It has to be considered that resolving such flow features requires a special high spatial and temporal resolution network. Possible evidence for an induced thermal circulation is presented in Burman et al. (1975) and is illustrated in Fig. 1a. The few surface-wind measurements along the irrigated area in southern Idaho show features which document a thermally induced circulation opposing a westerly synoptic flow. Voronstov (1963), based on pilot balloon wind measurements in the irrigated area of Pakhta–Aral, concluded that, in the summer, a local circulation often develops in the daytime over the area as evidenced there by southerly winds blowing most frequently at low altitudes, and northerly winds at the higher altitudes (above 700 m). The data from CINDE aircraft measurements in northeast Colorado suggest a change of wind velocity between the irrigated area and the surrounding dryland. Clear evidence for a significant thermally induced flow is absent in those observations, apparently due to the impact of the daytime induced upslope flows in that area.

3. Vegetation and soil surface thermal balance

In this section the sensible heat flux, the latent heat flux, the Bowen ratio, and the surface temperature of

the canopy and the soil surface, are evaluated. General features of these variables and their variability are provided, in addition to observational evaluations of their typical magnitude. These evaluations, which are based on various documented work, are oriented toward an estimation of the thermal forcing pertinent to the present study. Using this information and the analytical evaluations suggested in section 4 should provide a bulk estimation of their influence on the mesoscale circulations considered in the present study.

a. General evaluation

Using the surface heat balance equation, the sensible heat flux, H_s, from a dense vegetative surface can be approximated as

$$H_s = -E + \mathrm{LR}_N + (1 - a - t)R_s - \mathrm{PR} \quad (1)$$

where

- E latent heat flux which consists of contributions from leaf transpiration and possibly evaporation of intercepted droplets on the canopy
- LR_N net long wave radiation
- R_s incoming short wave radiation at the surface
- a albedo
- t transmissivity of the short wave radiation within the canopy
- PR photosynthesis and respiration fluxes.

Since PR is small in its magnitude as compared to the other terms in (1) it is generally neglected. The availability of thermal energy is determined by the net radiation terms.

For a bare soil surface, the sensible heat flux is given by

$$H_s = -E + \mathrm{LR}_N + (1 - a)R_s - G \quad (2)$$

where G is the soil thermal flux.

The incoming atmospheric long wave radiation at either a canopy surface or an adjacent bare soil area is almost identical. The outgoing long wave radiation emitted by a canopy is generally somewhat smaller than that of a bare soil surface, mostly when the soil surface is dry (in most cases, the canopy temperature is lower by at least several °C). Typical values of the net long-wave radiation, LR_N, for various crops during the daytime, as reported in Monteith (1975), are in the range of -60 to -125 W m^{-2}. Corresponding values of LR_N over a wet bare soil area are similar to those of vegetated surfaces; however, LR_N is larger in magnitude for bare dry soils. The difference in the solar radiation absorption between the two surfaces depends on their albedo and transmissivity. Typical canopy albedo values are in the range 0.1–0.3, and the range for bare soil surfaces is 0.05–0.4 (e.g., Davis and Idso 1979; Hillel 1982). While the solar radiation transmissivity in soil is obviously 0, the corresponding value for the canopy is related to the leaf density. The transmissivity of a single leaf is typically ~0.25 (e.g., Lee 1978). Typical values of transmissivity for the whole canopy layer as dependent on growth stage and sun zenith angle for various vegetation species are provided in Monteith (1976).

In grass or field crops, the daytime storage of heat in the canopy can be neglected (e.g., Tanner 1960). This may not be the case with a dense forest canopy, however. Review of studies evaluating bare soil surface thermal fluxes reported in Brutsaert (1982) suggests values of 30% with respect to the net radiation to be representative for the daytime soil heat fluxes, G.

Based on these evaluations, the sensible heat flux can be grossly related for dense vegetative surfaces (at least for scaling purposes) to its partition with the latent heat flux, based on the available net radiation ($R_{\mathrm{net}} = (1 - a - t)R_s + \mathrm{LR}_N$). Equations (1) and (2) can be rewritten respectively as

$$H_s \approx R_{\mathrm{net}} - E \quad \text{(dense vegetative surface)} \quad (3a)$$

$$H_s \approx R_{\mathrm{net}} - E - G \quad \text{(bare soil)}. \quad (3b)$$

Thus, estimating the net radiation together with the evapotranspiration (and the soil surface thermal flux when bare soil is considered), results in an estimation of the sensible heat flux (for scaling of the studied circulations in the present paper). For example, the clear sky daily solar radiation in subtropic and midlatitude locations during midsummer is around 25–30 MJ m^{-2} day^{-1}; e.g., see Duffie and Beckman (1974). This amount corresponds to a canopy evapotranspiration of about 7.2–8.8 mm day^{-1} when assuming $a = 0.2$, $\mathrm{LR}_N = -60$ W m^{-2} ($\mathrm{LR}_N \approx -2.6$ MJ m^{-2} day^{-1}) and $H_s = 0$. Daily estimates of canopy evapotranspiration can be used with the assumption of a daytime sinusoidal variation of R_{net} in order to provide temporal variations of H_s. Since canopy evapotranspiration is indirectly of considerable importance in the forcing of the mesoscale circulations discussed in this paper, its main features are outlined in the next subsection. The orientation of these outlines is to enable qualitative evaluation of the possible impact of vegetated surfaces on these circulations under various typical conditions.

The evapotranspiration rate for canopies can be composed of

- evaporation of intercepted water on the foliage due to rain or irrigation;
- evaporation from the soil beneath the canopy; and
- transpiration.

The first situation can be perceived as an evaporation from a water surface (when the leaves are wet their stomatal transpiration stops). For such a situation, a low sensible heat flux from the canopy to the atmosphere, or even a reversed flux (i.e., Bowen ratio < 0), is expected. The maximum magnitudes of intercepted water for various canopies, as reported by Rutter

(1975), are in the range of 0.5–2.1 mm day^{-1}. Thus, following a summer daytime shower on vegetated mountain slopes, for example, thermally induced upslope flows are likely to be suppressed (at least temporarily) due to enhanced evaporation and corresponding reduction of the sensible heat flux at the canopy surface.

Leaf transpiration through stomata is generally the major source of water vapor fluxes over dense vegetated areas. It is controlled by the stomatal aperture which is affected by (i) environmental conditions, (ii) vegetation characteristics, and (iii) soil water availability in the root zone.

1) ENVIRONMENTAL CONDITIONS

Transpiration rates from a canopy are influenced by the conductance of water from the soil root zone through the foliage to the atmosphere. There are five important environmental variables which regulate the conductance at a particular time: incident global radiation, leaf temperature, vapor pressure difference (VPD) between the leaf and the ambient air, ambient CO_2 air concentrations (the CO_2 impact is of only minor importance in the present study), and the soil water potential in the root zone (e.g., Jarvis and Morrison 1981). Figure 2 presents a schematic response of the stomatal vapor conductance (decreasing values of conductance indicate tendency toward stomatal closure) to these variables. From the aforementioned schematic description it follows that a very warm and dry surface layer results in a reduced stomatal vapor conductance and transpiration. Consequently, an increase in sensible heat flux occurs (as illustrated by the model simulation results presented in Figs. 8b–c and discussed in subsection 6a(3) of this paper.) A similar effect is caused by water stress (i.e., a deficit in soil wetness in the root zone which causes a reduced water transfer through the stomata of the leaves). Quantitative relations to account for the effect of the aforementioned forcings on the amount of transpiration are provided (at various degrees of refinement) in many studies (e.g., Szeicz et al. 1973; Kaufmann 1984; Avissar et al. 1985; Sellers et al. 1986, among others). Major factors affecting the magnitude of transpiration will be taken into account in the evaluation of the mesoscale circulations later in this study. Procedures to include these effects in our model evaluations are described in section 5.

2) VEGETATION CHARACTERISTICS

The vegetation characteristics relating to the transpiration rates include factors such as (i) leaf area index, LAI, i.e., the ratio of leaf area (one side) to the soil area underneath; (ii) shielding factor, σ_f, defined as the ratio between the area covered by canopy and the total area of the considered domain ($\sigma_f = 0$ for bare soil; $\sigma_f = 1$ for a completely covered surface; (iii) stage of growth as reflected by (i) and (ii); and (iv) leaf age. For an agricultural crop in the germination and seedling stage (generally in spring–early summer) both σ_f and LAI are low; thus in the beginning of the growing season a cultivated area resembles a bare soil. New leaves (typical for the first half of the growing season) transpire effectively, while in aging leaves, the transpiration rate is reduced or even eliminated.

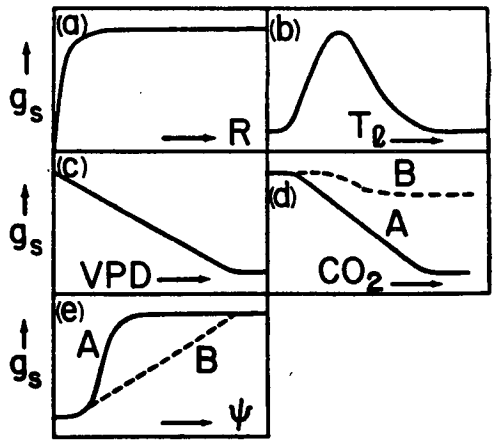

FIG. 2. The response of stomatal vapor conductance (g_s) to (a) solar radiation flux (R), (b) leaf temperature (T_l), (c) leaf-air vapor pressure difference; i.e., vapor pressure deficit (VPD), (d) mean intercellular space CO_2 concentration (CO_2), and (e) cell water pressure potential in the leaves (Ψ) (reflecting soil wetness conditions). (Adopted from Jarvis and Morison 1981).

3) SOIL WETNESS IN THE ROOT ZONE

Low water in the root zone is a common cause of stomatal closure and a cessation of the transpiration (water stress). Generally, the effective water intake depth for crops is less than 1 m for short vegetation (e.g., Danielson 1967), while it can be 1.5 m or deeper for trees and large shrubs. Hence, transpiration can occur even when the upper layer of the soil is dry. On the other hand, bare soil evaporation is practically eliminated once the upper surface layer of the soil becomes dry. Consequently this may lead, in many cases, to a significant thermal contrast between adjacent bare soil and vegetated areas [see, e.g., Case C3 in section 6a(2)].

b. Observational evaluations of surface fluxes over canopy

Table 1 presents selected examples of seasonal latent heat flux, E, evaluated from observations for common crops and grasses in the United States. It should be noted that these measurements do not always represent relatively large uniformly vegetated areas (an aspect which in general cannot be verified from the reports).

TABLE 1. Selected examples of typical observed warm season evapotranspiration for well watered common crops in the United States; see also Fritchsen (1982), (the approximated net radiation values were added by the authors of the present paper).

Crops	Location	Period of measurement	Observed evapotranspiration (mm day^{-1})	Approximated net radiation (in terms of evaporation) (R_{net}) (mm day^{-1})	Reference
Alfalfa	Kimberly, ID	1 May–30 Sep (69–71)	6.0	7.2	Jensen (1973)
Apples	Wenatchee, WA	1 Apr–31 Oct (55, 57–59)	7.0	6.0	Jensen (1973)
Barley	Powell, WY	18 May–16 Aug (56–57)	4.3	7.2	Jensen (1973)
Beans	Powell, WY	28 May–3 Sep (57)	5.9	7.2	Jensen (1973)
Beans	Davis, CA	21 June–24 Sep (68)	4.3	5.7	Jensen (1973)
Bermuda	Raleigh, NC	30 May–22 Sep (58)	3.9	5.7	Jensen (1973)
Bermuda	Mesa and Tempe, AZ	16 Apr–15 Oct (59–60, 63–64)	6.0	6.8	Jensen (1973)
Cantaloupe	Mesa, AZ	1 Apr–15 Jul (59–62)	4.6	7.5	Jensen (1973)
Castrobean	Mesa, AZ	15 Apr–15 Nov (58)	7.5	6.2	Jensen (1973)
Corn	Powell, WY	30 May–6 Sep (58–60)	4.2	7.2	Jensen (1973)
Corn	Coshocton, OH	23 May–25 Sep (61)	3.8	5.0	Jensen (1973)
Corn	Bushland, TX	7 May–8 Sep (70)	5.0	6.5	Jensen (1973)
Corn	Davis, CA	15 May–20 Sep (70–71)	5.0	6.5	Jensen (1973)
Cotton	Mesa and Tempe, AZ	1 Apr–15 Nov (54–62)	7.6	6.5	Jensen (1973)
Rice	Davis, CA	1 May–30 Sep (68–69)	6.1	5.6	Jensen (1973)
Sorghum	Mesa, AZ	1 Jul–31 Oct (55–58, 60)	3.6	7.0	Jensen (1973)
Soybean	Mesa, AZ	16 Jun–31 Oct (44)	4.1	7.0	Jensen (1973)
Sugar beet	Huntley, MT	20 Apr–27 Sep (53)	5.2	5.4	Jensen (1973)
Sugar beet	Kimberley, ID	15 Apr–17 Oct (65–67)	3.4	6.7	Jensen (1973)
Sugar beet	Davis, CA	25 Mar–20 Sep (66)	4.6	4.9	Jensen (1973)
Sugar beet	Garden City, KS	10 Apr–1 Nov (59–60)	5.8	5.6	Jensen (1973)
Sugar beet	Bushland, TX	28 Mar–18 Oct (64, 66)	6.2	5.5	Jensen (1973)
Sugar beet	Mesa, AZ	1 Oct–17 Jul (65–66)	4.1	5.3	Jensen (1973)
Safflower	Kimberley, ID	1 Apr–30 Sep (66)	3.5	5.7	Jensen (1973)
Tomato	Davis, CA	30 Apr–24 Sep (69)	3.1	5.6	Jensen (1973)
Wheat	Sidney, MT	4 Apr–16 Aug (78)	4.7	6.0	Aase and Siddoway (1982)
Wheat	Sidney, MT	5 May–17 Aug (79)	5.5	6.2	Aase and Siddoway (1982)

In relatively small vegetated areas, advection of warmer and drier air from the surroundings is likely to increase the evapotranspiration (sometimes significantly) as compared to the case of larger areas. The approximated net radiation computations are based on solar radiation averages adopted from Duffie and Beckman (1974) and while assuming an albedo value of 0.2 and $LR_N = -2.6$ MJ m^{-2} day^{-1}.

Reviewing Table 1 suggests that, grossly over vegetated areas, more than 70% of the estimated typical net radiation for the stated periods is converted to latent heat flux, and thus less than 30% is converted to sensible heat flux. Over relatively dry areas of bare soil, however, evaporation rates can be very low, even zero. Therefore, in this case, a considerable amount of the net radiation is converted to sensible heat flux. A configuration of adjacent areas of bare soil and vegetation is likely to exist in relatively dry geographical locations, and should have the potential to induce thermally direct circulations. In a similar configuration except with a relatively wet bare soil, evaporation fluxes can approach that of the evapotranspiration in a cultivated field (e.g., Jensen 1973) and therefore significant thermally-forced circulations would not be expected (see Case C1, Fig. 5c for a model simulation of this situation).

Table 2 presents the contrast in evaporation rates from adjacent crops and fallow areas evaluated based on several simultaneous measurements. Typically the evapotranspiration rate over a vegetated area is higher by at least 2 mm day^{-1}, than over the bare soil.

The values of E from forest canopies during the warm season in various geographical locations are given in Table 3. Typically the values of E in wet soil areas (i.e., with high rainfall) are smaller by at least 1–2 mm day^{-1} as compared to the well irrigated crops outlined in Table 1. In geographical locations with a low rainfall (or extended drought during the warm season) E becomes quite small.

In some studies the Bowen ratio ($\beta = H_s/E$) is reported, providing the possibility for a better estimation of the sensible heat flux, H_s. From Eqs. (3a) and (3b), H_s can be approximated as

$$H_s \approx \frac{R_{net} - G}{1/\beta + 1} \tag{4}$$

with $G = 0$ for vegetated surfaces.

Typical values of the Bowen ratio during the warm season for various vegetation types are provided in Table 4. Wet canopies have significantly lower Bowen ratios than dry canopies.

TABLE 2. Selected examples of evapotranspiration fluxes from adjacent vegetated and fallow areas during the warm season.

Soil type	Vegetation	Location	Period	Evapotranspiration (mm day^{-1}) Vegetation	Soil	Reference
clay-loam	wheat	Swift Current Sask., Canada	May (germination)	3.3	3.4	Reddy (1983)
clay-loam	wheat	Sask., Canada	1–22 Jun	5.0	2.3	Reddy (1983)
clay-loam	wheat	Sask., Canada	23 Jun–20 Jul	3.8	1.1	Reddy (1983)
silt loam top, forest clay bottom	wheat	Koen Forest, AR	1 May–1 Jul 1970	4.5	2.6	Rogerson (1976)
—	wheat	Sidney, MT	20 Jun–17 Aug 1979	4.5	0.9	Aase and Siddoway (1982)

Figure 3 presents the daytime peak values of the sensible and latent heat fluxes involved with various types of canopies at different months of the warm season. Typical latent heat fluxes are generally substantially larger than the sensible heat fluxes particularly during the midsummer (i.e., $\beta < 1$). At that time a considerable portion of the net radiation is converted into latent heat fluxes. Irrigated crops showed higher values of latent heat fluxes as compared to nonirrigated vegetation. The averaged values obtained over the Amazonian rain forest during synoptically undisturbed and clear days at the end of July are worth noting. These values were observed at a site representing an extended forested area.

4. Analytical evaluations

In order to provide a general qualitative insight into the pertinent features of mesoscale circulations considered in the present study, an analytical evaluation is carried out, which is based on the circulation theorem and follows the procedures used in Ookouchi et al.

TABLE 3. Selected examples of observed evapotranspiration from forests during the growing season throughout the world; see also Fritchsen (1982).

Species	Soil wetness/location	Evapotranspiration (mm day^{-1})	Reference
	Negligible soil water deficit		
Eucalyptus niphophia	New South Wales, Australia	3.8	Rutter (1968)
Douglas fir	Haney, British Columbia	~7.0	Black (1979)
	Small soil water deficit		
Picea abies (wet site)	Scania, Sweden	4.8	Rutter (1968)
Pinus resinos and Quercus	Lower Michigan	2.8	Rutter (1968)
Populus tremuloids	Gunnison, Colorado	4.2	Rutter (1968)
Pinus Contoria	Fraser, Colorado	1.5	Rutter (1968)
	Moderate soil water deficit		
Pinus echinata and Quercus	New Jersey	3.0	Rutter (1968)
Populus Tremuloides	Farmington, Utah	3.9	Rutter (1968)
Pinus echinata and Quercus	Vinton, Ohio	3.5	Rutter (1968)
Shrubs	Vinton, Ohio	3.2	Rutter (1968)
Pinus taeda	Union, S. California	3.7	Rutter (1968)
Qurecus	Crossett, Arkansas	4.2	Rutter (1968)
Pinus echinata and pinus taeda	Crossett, Arkansas	4.5	Rutter (1968)
	Severe soil water deficit		
Maqui Shrubs	Carmel, Israel	1.9	Rutter (1968)
	Extreme soil water deficit		
Quercus dumosa and other chaparral	San Dimas, California	1.9	Rutter (1968)
Douglas fir	Haney, British Columbia	0.8–1.8	Black (1979)

TABLE 4. Ranges of Bowen ratios for typical summer daylight hours for selected canopies.

Species	No. of days	Location	Bowen ratios: Wet canopy	Bowen ratios: Dry canopy, Overcast	Bowen ratios: Dry canopy, Sunny	Reference
Pinus radiata	3		—	—	0.1–0.8	
Pinus contorta	1		—	—	0.4–1.2	
Pinus taeda	—		0.1–0.4	0.4–1.4	0.4–1.4	
Picea sp.	19		0.2–0.4	0.2–2.1	0.3–1.2	
Pinus resinosa/strobus	5		—	0.45	0.6–2.0	
Pinus sylvestris	3		—	—	−0.1–0.8	Coniferous forests
Pinus sylvestris	4		—	0.2–0.7	0.3–3.5	
Pinus sylvestris	1		—	—	0.5–1.3	
Pinus sylvestris	8		−0.3	0.5–2	1–4	Based on studies referenced
Pinus sylvestris	7		—	—	−0.2–1.3	in Jarvis et al. (1976)
Pseudotsuga menziesii	3		—	0.3–0.4	0.3–1.8	
Pseudotsuga menziesii	6		—	0.5–1.6	0.2–1.5	
Picea abies	4		—	−0.3–1.3	0.2–3.1	
Picea abies	8		—	0.0–1.0	0.1–0.9	
Cotton	Seasonal	Texas	—	0.23		Ritchie (1971)
Cotton	Seasonal	Central Asia	—	0.07		Ritchie and Burnett (1971)
Cotton	Seasonal	Tempe, AZ	—	—	−0.3–1.0	Fritschen (1982)
Alfalfa	Seasonal	Tempe, AZ	—	—	−0.4–0.0	Fritschen (1982)
Wheat	Seasonal	Tempe, AZ	—	—	−0.2–0.0	Fritschen (1982)

(1984) and in Segal et al. (1986), with some additional refinements. The circulation paths in Fig. 4 broadly illustrate the types of mesoscale responses which interest us here: 1) circulations along flat terrain, and 2) circulations along slopes. In both cases the circulation path is assumed to occur between the surface and the top of the planetary boundary layer (PBL). The circulation segment along the top of the PBL grossly divides the opposing flows of the circulation (e.g., Anthes 1978), therefore the velocity along it is negligible and

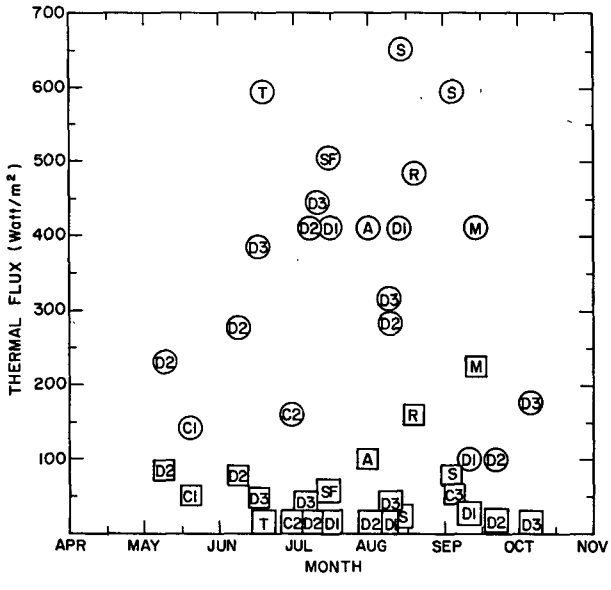

FIG. 3. Typical values of sensible heat (indicated by squares) and latent heat (indicated by circles) fluxes over canopy surfaces during the warm season as dependent on month for various vegetation types, based on various observational studies reported in Monteith (1976). The following vegetation types are considered: C1, C2 and C3—cotton; D1—mixed oak, maple and aspen area (12–19 years old); D2—natural oak forest (40–60 years old); D3—planted maple forest (40–60 years old); M—maize; R—rice; S—sugar beet; SF—sunflower; T—Townsville stylo. A—The Amazonian rain forest (from Martin et al. 1988).

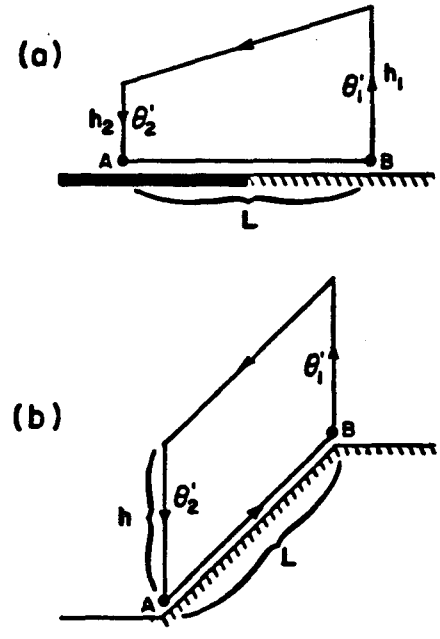

FIG. 4. Schematic of the chosen path of integration for the circulation evaluation: (a) along flat terrain with thermal differentiation, (the dark segment indicates a vegetated section); (b) along a single slope.

the contribution to the line circulation can be ignored. The lateral segments of the path in the flat terrain case correspond to the horizontal extent of the circulation (which varies with time). The contribution of the lateral segments to the line circulation is also ignored because of their reduced extent (as compared to the horizontal segment) as well as the reduced magnitude of the vertical velocity as compared to the horizontal velocity. For the slope case, the lateral sections of the circulation path are fixed with time at the bottom and top of the slope.

The circulation tendencies at the surface are given by the following relations:

(i) Flat terrain case:

$$\frac{\partial C_s}{\partial t} = \frac{\partial}{\partial t}\int_A^B u_s dl \approx \frac{g}{\theta}(h_1\tilde{\theta}'_1 - h_2\tilde{\theta}'_2) + \int_A^B F(u_s)dl; \tag{5}$$

(ii) Slope case:

$$\frac{\partial C_s}{\partial t} = \frac{\partial}{\partial t}\int_A^B u_s dl \approx \frac{g}{\theta}\frac{\partial\theta_0}{\partial z}\frac{\partial z_G}{\partial x}\cdot L\cdot h - (\tilde{\theta}'_2 - \tilde{\theta}'_1)\frac{g}{\theta}h + \int_A^B F(u_s)dl \tag{6}$$

where C_s is the line circulation along the surface between the points A and B; u_s is the surface wind component along the circulation path; h is the height of the PBL; L is the horizontal scale of the circulation; θ is the potential temperature; g is the gravitational acceleration; F is the frictional force; $\partial\theta_0/\partial z$ is the environmental potential temperature lapse; $\partial z_G/\partial x$ is the slope steepness; superscript ($\tilde{}$) indicates a vertically averaged quantity within the PBL depth and ($'$) designates a perturbation from an initial mean value.

For scaling purposes Tennekes' (1973) evaluation of the PBL height, h, at a given time t, is used:

$$h \approx \left[\frac{2\int_0^t H_s dt}{\rho_a C_p \dfrac{\partial\theta_0}{\partial z}}\right]^{1/2} \tag{7}$$

where H_s is the sensible heat flux at the surface, ρ_a is the air density and C_p is the air specific heat at constant pressure. Analogous to Eq. (7), as used in Segal et al. (1986), is the relation:

$$\tilde{\theta}'(t) \approx \frac{1}{2}h\frac{\partial\theta_0}{\partial z}. \tag{8}$$

The Rayleigh frictional form is adopted:

$$F(u_s) = -\alpha u_s. \tag{9}$$

Substituting values estimated by Eq. (7)–(9) into Eq. (5)–(6) and integrating with respect to time, provides the surface line circulations, as follows:

(i) Flat terrain case:

$$\int_A^B u_s dl = \frac{g}{\theta}(\rho_a C_p)^{-1}e^{-\alpha t} \times \int_0^t e^{\alpha\tau}\int_0^\tau [(H_{s_1} - H_{s_2})d\tau']d\tau \tag{10}$$

(ii) Slope case:

$$\int_A^B u_s dl \approx \sqrt{2}\frac{g}{\theta}\frac{\partial z_G}{\partial x}\left(\frac{\partial\theta_0}{\partial z}\right)^{1/2}(\rho_a C_p)^{-1/2}Le^{-\alpha t} \times \int_0^t\left[e^{\alpha\tau}\left(\int_0^\tau H_s d\tau'\right)^{1/2}\right]d\tau. \tag{11}$$

Comparisons of these analysis results and model simulation results provided in section 6d, help establish the validity and usefulness of these relations. In addition, utilizing information outlined in section 3, scaling can be obtained for the expected intensity of mesoscale circulations investigated in the present study.

An additional approach for scaling the impact of vegetation cover on related mesoscale circulations can be applied if the canopy surface temperature (and that of the soil, if relevant) is available. Utilizing linear model solutions, or alternatively, applying a numerical model forced by a prescribed surface temperature can provide further insight in that regard.

5. The numerical model

a. The atmospheric module

A numerical model, consisting of atmospheric, soil and plant modules, was used in order to provide a refined quantitative insight into the thermally forced circulations. The atmospheric module formulation is described comprehensively in Pielke (1974), Pielke and Mahrer (1975), Mahrer and Pielke (1977), Mahrer and Pielke (1978), and McNider and Pielke (1981). Validation of the model has indicated its skill to realistically resolve mesoscale fields (e.g., studies by Pielke and Mahrer 1978; Segal et al. 1982; and Abbs and Pielke 1986, among others).

Two versions of the soil-plant modules were adopted in the present study. Results obtained using the two versions were compared. A short description of their formulation is provided below.

b. Soil-plant module—version 1 (VER1)

This version is described in detail in McCumber (1980) and McCumber and Pielke (1981). The soil module consists of a prediction equation for the soil temperature as a function of depth (z):

$$c\frac{\partial T_s}{\partial t} = \frac{\partial}{\partial z}\left(\lambda\frac{\partial T_s}{\partial z}\right) \tag{12}$$

where T_s is the soil temperature; c is the soil volumetric heat capacity; and λ is the soil thermal conductivity.

In addition, a volumetric moisture prediction equation given as

$$\frac{\partial \eta}{\partial t} = \frac{\partial}{\partial z}\left(D_\eta \frac{\partial \eta}{\partial z}\right) + \frac{\partial K_\eta}{\partial z} + A(z) \qquad (13)$$

is included where η is the volumetric soil wetness, D_η is the moisture diffusivity, K_η is the hydraulic conductivity, (which reflects the water conduction due to gravity), and $A(z)$ is a function expressing water extraction by roots when vegetation is present. Determination of the matric potential (i.e., the potential of soil water due to capillary and adsorptive forces), the hydraulic conductivity and the moisture diffusivity follow the functional relations suggested by Clapp and Hornberger (1978). In the present study a constraint $D_\eta > 0.8 \times 10^{-5}$ cm^2 s^{-1} (as implied from observed values reported by De Vries, 1963) was introduced. In the solutions of (12) and (13) eleven different United States Department of Agriculture textural classes of soils and a peat soil can be specified. Heat and moisture balance equations are solved at the air–soil interface in order to provide the interface temperature and moisture.

The plant module adopted in VER1 is, in general, similar to that formulated by Deardorff (1978). It consists of solving a heat balance equation for a single canopy layer, in addition to the heat balance equation solved for the air–soil interface. The net balance equation for the canopy considers sensible and latent heat flux exchanges with the surrounding air, as well as the fluxes of short- and longwave radiation. The root extraction term in Eq. (13) is based on the study of Molz and Remson (1970) which relates the root extraction term $A(z)$ to the vertical distribution of the root.

The canopy stomatal resistance, which is a major factor determining the transpiration rate, is given in this version as

$$r_s = r_c\left[\frac{(R_s)_{\max}}{0.03(R_s)_{\max} + R_s} + \left[\frac{\eta_{\text{wilt}}}{\eta_{\text{root}}}\right]^2\right] \qquad (14)$$

where $(R_s)_{\max}$ is the daily maximum net solar radiation under a cloudless sky and R_s is the incoming solar radiation, at the canopy top; η_{wilt} is the volumetric soil wetness which would result in permanent wilt conditions; and η_{root} is the soil volumetric wetness at the root zone. The term r_c is a resistance coefficient dependent upon plant type [based on Eq. (14), for relatively wet soils around noon, $r_c \approx r_s$]. Typical values of r_s around noon during the summer season in the midlatitudes for crops is about 2 s cm^{-1} (e.g., see Monteith 1976) which was adopted in the simulations which used VER1.

c. *Soil-plant-lower atmosphere—version 2 (VER2)*

A detailed description of the formulation involved with VER2 is given in Avissar et al. (1986), and Avissar and Mahrer (1988). Only a general outline is provided here.

As in VER1 both soil thermal diffusion and soil moisture equations are solved. The thermal properties of soil, however, are computed following a procedure suggested by De Vries (1963) while the hydraulic parameters are estimated according to Kozeney and Carmans' approach (Wyllie and Gardner 1958). The soil formulation is provided in detail in Mahrer et al. (1984), Avissar and Mahrer (1982, 1986, 1988), and Mahrer and Avissar (1985). Validation results reported in these studies indicated the skill of the soil scheme to resolve the soil temperature and moisture profiles.

The main difference between VER1 and VER2 consists in the parameterization of the sensible and latent heat fluxes from the soil and the vegetation to the atmosphere. The drag coefficients, limited in VER1 to be actually valid only near neutral surface layer conditions are removed, and in VER2 the effects of the soil–vegetation system are directly incorporated into the Businger et al. (1971) equations which are used to describe the atmospheric surface layer of the model. The latent and sensible heat fluxes are formulated as follows (v indicates vegetative surface; g indicates soil surface):

$$\begin{aligned} E_v &= \sigma_f' \rho L u_* q_* \\ E_g &= (1 - \sigma_f')\rho L u_* q_* \\ H_v &= \sigma_f' \rho c_p u_* \theta_* \\ H_g &= (1 - \sigma_f')\rho c_p u_* \theta_* \end{aligned} \qquad (15)$$

where ρ, L and c_p are, respectively, the air density, the latent heat of evaporation and the specific heat at constant pressure. The variables u_*, q_* and θ_* are, respectively, the surface friction velocity, the flux humidity and the flux temperature (the formulation in Businger et al. 1971 is used for their computation). The term σ_f' expresses the relative contribution of the vegetation to the total heat fluxes between the surface (composed of one surface of soil and 2 LAI $\sigma_f \epsilon$ surfaces of vegetation) and the atmosphere. It is defined as follows:

$$\sigma_f' = \frac{2 \text{ LAI } \sigma_f \epsilon}{1 + 2 \text{ LAI } \sigma_f \epsilon} \qquad (16a)$$

where LAI is the leaf area index of the vegetation and σ_f is a shielding factor which represents the fractional coverage of the ground by canopy. The ϵ factor (assumed to be constrained by $1/\text{LAI} \leqslant \epsilon \leqslant 1$; in the present study $\epsilon = 1$ is adopted) provides a measure of the effectiveness of the canopy surfaces to contribute to the heat and moisture fluxes. The value of σ_f' is near unity for a completely vegetated surface and 0 for a bare soil. Equation (16a) is used in cases where a given model grid cell is covered entirely by vegetation (i.e., $\sigma_f = 1$) or when it is covered uniformly throughout the

whole grid cell by vegetation which is not dense (e.g., $\sigma_f < 1$ due to row intervals in crops). When in a given model grid area it is assumed that a specific fraction σ_f is covered completely with a dense vegetation while the other fraction is a bare soil, the following relation is used:

$$\sigma'_f = \sigma_f. \tag{16b}$$

Using this formulation for the latent heat fluxes, the surface specific humidity, q_{z_0}, required for the computation of q_*, is

$$q_{z_0} = \sigma'_f q_v + (1 - \sigma'_f) q_g \tag{17}$$

where q_v, the specific humidity of the leaf surface, is computed following a procedure suggested by Avissar et al. (1985). This procedure accounts for the leaf stomata reaction to (i) solar global radiation, (ii) leaf temperature, (iii) VPD between leaf and ambient air, (iv) CO_2 concentration, and (v) soil water potential in the root zone. The response functions derived in Avissar et al. (1985) were adopted (however, in case study simulations where specific vegetation species are involved, the response function should be calibrated based on the characteristics of the involved vegetation type).

The soil surface specific humidity, q_g, is computed following Avissar and Mahrer (1986) as

$$q_g = s_w q_{g_v} + (1 - s_w) q_{z_0} \tag{18}$$

where q_{g_v} is the upper soil layer specific humidity calculated according to Philip and De Vries (1957), and s_w is a surface wetness function which depends upon soil type and water moisture content.

Similarly, the surface potential temperature, θ_{z_0}, required for the computation of θ_*, is given by

$$\theta_{z_0} = \sigma'_f \theta_v + (1 - \sigma'_f) \theta_g \tag{19}$$

where θ_v and θ_g are, respectively, the vegetation and soil surface potential temperatures.

6. Model calculations

Several two-dimensional model simulations were carried out under clear sky conditions in order to evaluate the impact of vegetation cover on typical daytime thermally induced mesoscale circulations (i.e., sea breeze and thermally induced upslope flows) and the generation of such circulations due to heterogeneities in the surface vegetative cover. The simulated cases are based on a prescription of input parameters such as vegetation type, soil type, and their distribution. The selection of the simulated cases was designed to be useful in interpreting actual meteorological situations in specific geographic areas. Most of the simulations were performed with the VER2 version of the soil-plant modules, however, two comparisons using the VER1 modules were made, in order to support the generality of the simulation results. In the simulations, unless stated otherwise, Eq. (16a) was adopted for the definition of σ'_f.

The simulations commenced at 0800 LST which corresponds to the time when the sensible heat fluxes typically become effective in the development of the convective PBL on sunny days. Table 5 provides pertinent model parameters involved with the presented simulations. The initial vertical profiles of the potential

TABLE 5. Model input parameters and initial conditions.

Surface roughness	land	4 cm
	grass	10 cm
	trees	100 cm
Bare soil albedo		0.2
Vegetation albedo		0.2
Initial surface temperature		27°C
Initial potential temperature lapse $\frac{\partial \theta_0}{\partial z}$		3.5°K/1000 m
Synoptic flow		calm (unless otherwise specified)
Integration time step		60 s
Horizontal grid interval		3 km
Latitude		32°
Day of the year		August 15
Soil type		clay-loam
Vegetation LAI		3.0

Root fractional distribution with depth

Depth below surface (cm)	1	2	3	4	5	8	13	20	30	50	75	100
Root fraction	.01	.01	.05	.06	.06	.09	.11	.15	.15	.15	.16	.00

Initial specific humidity, q

Height (km)	.005	0.015	0.03	0.06	0.1	0.2	0.4	0.7	1.0	1.5	2.0	2.5	3.0	3.5	4.0	4.5	5.0	6.0	7.0
q (g kg^{-1})	10	10	10	10	10	10	10	10	8	6	2.5	1.5	1	.5	.5	.5	.5	.5	.5

TABLE 6. Description of the simulated flat terrain cases (* indicates use of VER1). Vegetation type 1 indicates trees; vegetation type 2 indicates crops.

Case	Volumetric soil wetness (%) West	Volumetric soil wetness (%) East	/Vegetation type/σ_f/LAI/ West	/Vegetation type/σ_f/LAI/ East	Figure
		General case simulations			
SBS	water	5	—	—	5a
SBV	water	25	—	/2/1/3/	5b
C1	25	25	/2/1/3/	—	5c
C2	25	5	/2/1/3/	—	6a
C2*		as C2 except for using VER1			6b
C3	5% in the upper 5 cm, 25% below	5% in the upper 5 cm, 25% below	/2/1/3/	—	6c
C4	5	5	/2/1/3/	—	7a
C4*		As C4 except for using VER1			7b
C5	the same as Case C3 except for $\sigma_f = 0.25$ (using Eq. (16b) for σ_f')				7c
		Oasis simulations			
C6	Same as C2 except for vegetation in the middle of the domain				10a
C7	Same as C6 except for $\sigma_f = 0.25$ (using Eq. (16b) for σ_f')				10b
C8	Same as C6 except for a synoptic geostrophic flow of 3 m s^{-1}				10c

temperature (θ) ($\partial\theta_0/\partial z = 0.0035°K\ m^{-1}$) and the specific humidity (q) as given in Table 5 reflect summer conditions in the subtropical regions.

a. Flat terrain simulations—influence of vegetation

The general characteristics of the set of simulations involved with this category are outlined in Table 6. For all the simulations the soil type was assumed to be clay-loam with a basic initial volumetric wetness of 5% for dry soil and 25% for wet soil. All the simulated fields [including the component of the wind along the cross section, u (east–west), the vertical velocity w, the potential temperature θ, and the specific humidity q, as well as the surface sensible, H_s, and latent heat fluxes, E] are presented for 1400 LST when the involved circulations are in their mature stage. Clear sky conditions are assumed in the simulations.

1) SEA BREEZE CASES

Two sea breeze simulations were performed, one with a dry bare soil (Case SBS) and the other with wet soil covered with dense vegetation ($\sigma_f = 1$, Case SBV). These simulations are designed to illustrate the impact of vegetative cover on the intensity of the sea breeze as well as to provide a control case to which the other simulations may be compared. Figure 5a provides the simulated field of the wind u component at 1400 LST for the Case SBS. The v component (the south–north flow component) at this hour is about 0.15 u and thus is not of significance for illustration purposes. Only later in the day does its intensity increase significantly as a result of the Coriolis effect. The SBS simulation provides a situation with a large horizontal gradient in the sensible heat flux leading to a strongly developed sea breeze circulation by that hour as indicated by the intensity of u, w and the thermal contrast implied by the θ field. The q field indicates relatively low values of well mixed moisture within the inland PBL.

Investigation of the impact of vegetation cover on the intensity of the south Florida summer sea breeze was carried out by McCumber (1980) using a three-dimensional version of the model. He found a pronounced effect on the sea-breeze intensity when the natural vegetation was eliminated in a model simulation. As anticipated, increased evapotranspiration in Case SBV (Fig. 5b) led to a reduction in H_s. Consequently, the sea-breeze intensity was reduced significantly in intensity (peak values of u and w within the simulated cross section are reduced to around 2 and 3 cm s^{-1}, respectively). Suppression of H_s also resulted in a retardation in the development of the inland PBL, a related reduction in the heating in the θ field and an increase in its moisture content. It is worth noting that in a study of summer daytime flow intensity and maximum air temperature in the coastal area of Israel (where the flow consists mostly of the sea breeze), Alpert and Mandel (1986) found a trend of a reduction in both of these variables during the last 40 years. These authors attributed the reduction in part to the trend of an increase in irrigation and vegetated areas in coastal Israel during this period.

2) BARE SOIL-VEGETATED SOIL CONTRAST (NONSTRESSED TRANSPIRATION CONDITIONS)

Contrasting an area with relatively wet soil with a region of nonstressed vegetation (imposed by high soil

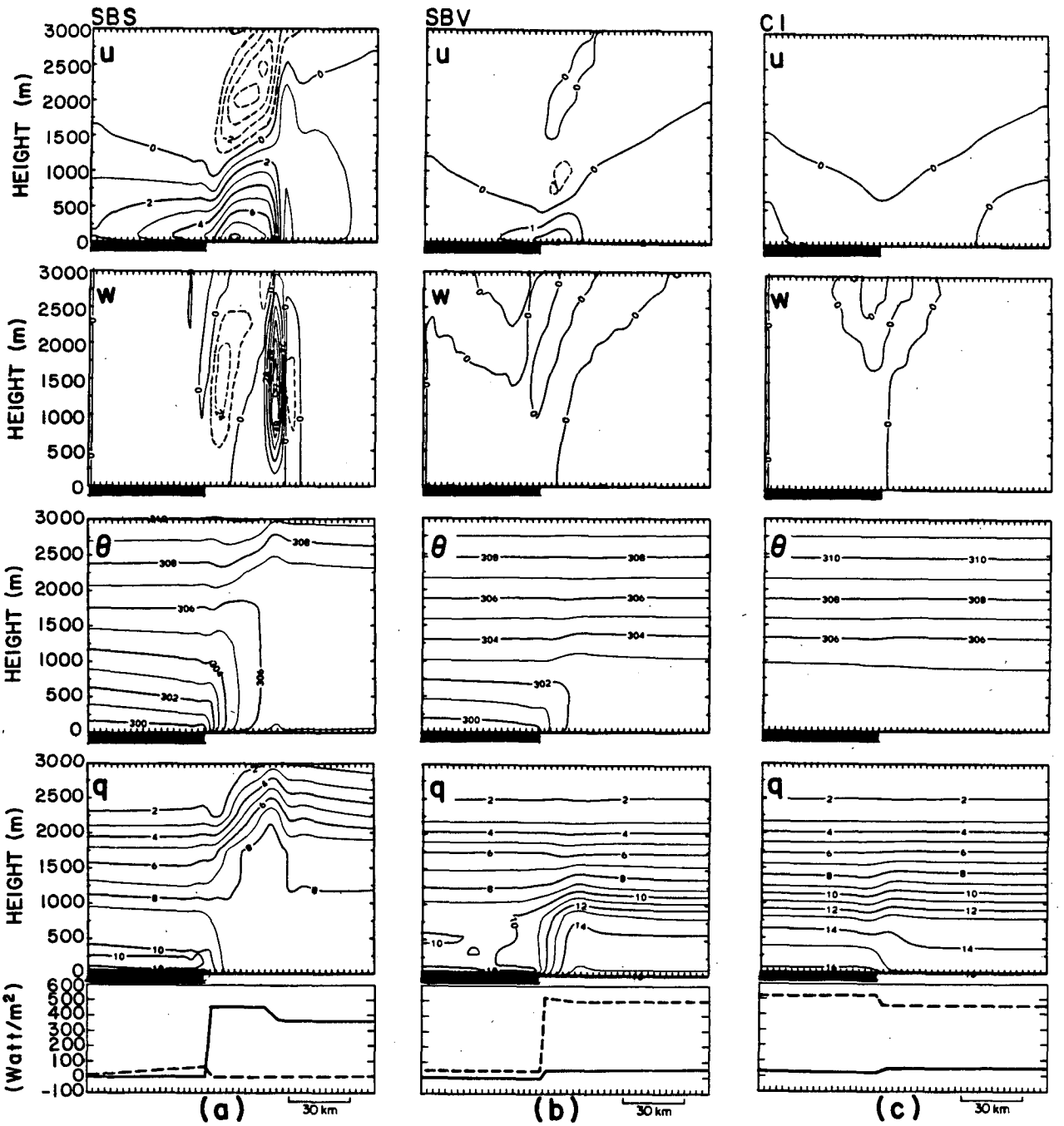

FIG. 5. Vertical cross section of the simulated domain for the Cases SBS, SBV (where the dark segment indicates the sea) and C1 (where the dark segment indicates the vegetation section), (see Table 6 for the case descriptions) at 1400 LST for (i) u—west–east component of the wind in m s^{-1} (dashed contours indicate negative component-easterly), (ii) w—vertical wind component in cm s^{-1} (dashed contours indicate negative component-downward vertical velocity), (iii) θ—the potential temperature in K, (iv) q—the specific humidity in g kg^{-1}, (v) the sensible (solid line) and latent (dashed line) heat fluxes at the surface.

moisture content in the vegetated area) results in the generation of only a minor circulation (Case C1; Fig. 5c). This circulation pattern resembles that obtained in the case SBV. It generally agrees with the observation that evaporation from wet bare soil and evapotranspiration from vegetation are similar, thus sensible heat fluxes into the atmosphere are also expected to be similar over both surfaces. The situation represented in Case C1, for example, could follow a regional rain event which increases soil wetness over both types of areas.

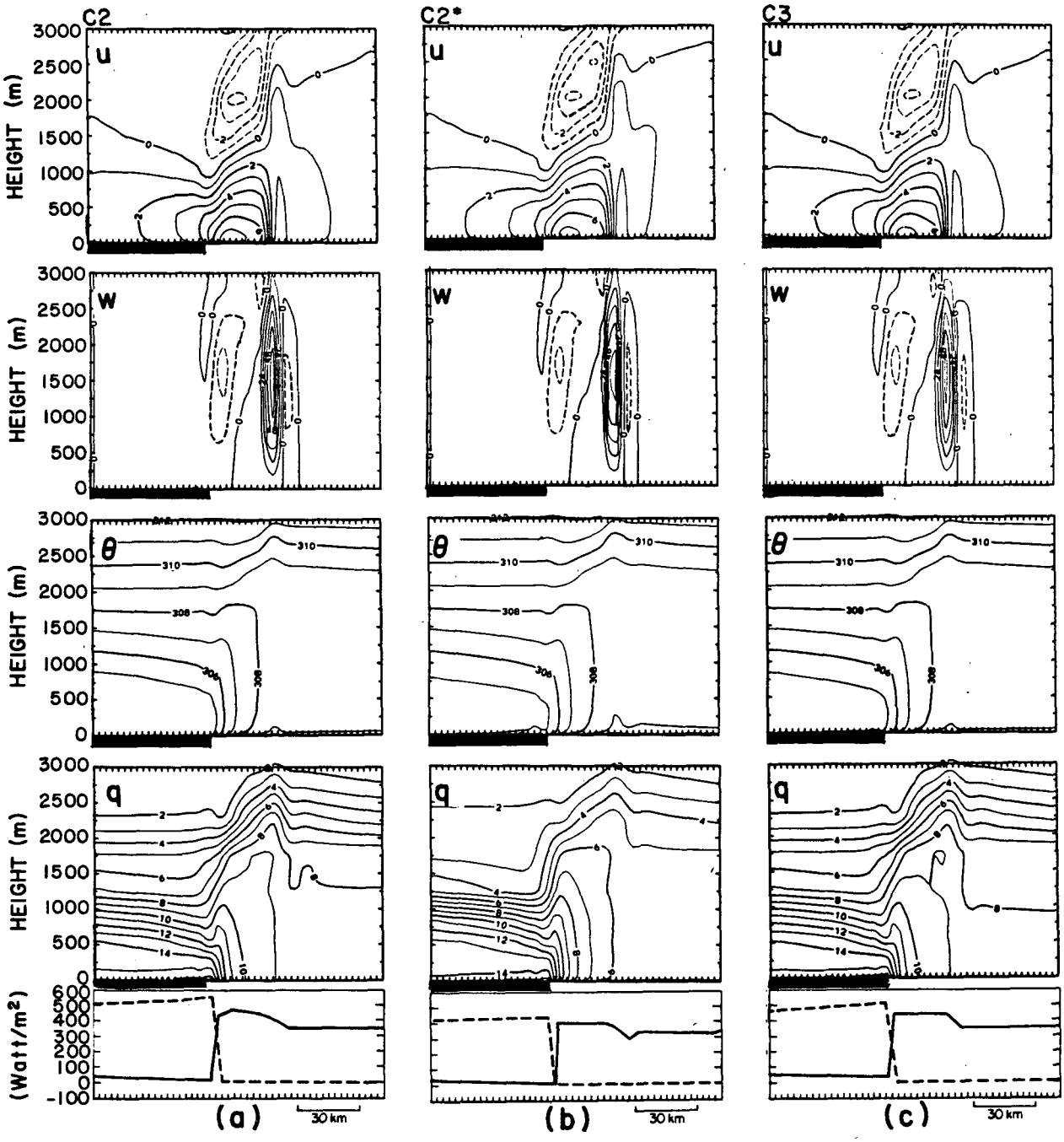

FIG. 6. As in Fig. 5, except for Cases C2, C2* and C3 (the dark segment indicates the vegetation section).

Contrasting, however, a nonstressed vegetation with a dry bare soil (Case C2; Fig. 6a) results in the generation of a more intense circulation due to a strong horizontal gradient in H_s. The peak values of u (7 m s^{-1}) and w ($\sim$60 cm s^{-1}) for Case C2, as well as the horizontal extent of the circulation, are generally similar to those obtained in Case SBS. A shallow PBL develops over the vegetation segment as is evident from the θ field. Enhanced evapotranspiration over the vegetated segment provides a supply of moisture which significantly increases the water vapor in the shallow PBL segment. As with the SBS case, the moisture is advected by the thermally induced flow toward the dry bare soil segment, where it becomes well mixed within the relatively deep convective PBL. It is worth noting that in the present case the vegetated surface was transpiring at a potential rate which was greater than the evaporation from the sea in case SBS. This is due to

larger aerodynamic roughness and the predicted higher canopy temperature (~33°C while the stomata were entirely opened) as compared to the imposed sea surface temperature in SBS (27°C).

Case C2* (Fig. 6b) is identical to Case C2 except for using the VER1 module of soil/vegetation. Comparing the meteorological fields obtained in Case C2* with those of Case C2 indicate good agreement, thus further supporting the credibility of the simulation results.

The next experiment (Case C3) explores the case when a precipitation event occurs over a vegetated region adjacent to a bare soil region. For some period of time following the event both areas are anticipated to have relatively large evaporation. Eventually, however, the upper layer of the soil dries and, consequently, the evaporation from the soil surface significantly decreases (although the soil below remains relatively wet). In the vegetated area, however, the root-zone moisture uptake maintains the supply of water for the evaporative fluxes which would not exist without a vegetative cover (for example, see model evaluations by Pan and Mahrt 1987). Case C3 provides an illustration for such a situation where the soil is permitted to dry out at the surface (see Table 6 for a specification of the initial moisture profile). Simulation results obtained in this case are presented in Fig. 6c showing similar features for the u, w, θ and q fields as obtained in Case C2. It appears, therefore, that "deforestation" in Case C3 would lead to (i) an elimination of significant evaporative fluxes into the atmosphere after the soil surface dries out and (ii) the elimination of the thermal circulation and its convergence zone. The evaporative fluxes and the low-level convergence are supportive for the initiation of convective clouds under favorable synoptic conditions. On the other hand enhanced evaporative fluxes are associated with the suppression of the PBL daytime development and could contribute to a retardation of convective development.

3) BARE SOIL-VEGETATED SOIL CONTRAST (REDUCED TRANSPIRATION CONDITIONS)

As discussed in section 3, reduced soil wetness as well as environmental conditions leading to increased leaf temperature (e.g., due to warm ambient air, high solar radiation, etc.) tend to lead to various degrees of stomatal closure. Thus a reduction in the transpiration rates under such extreme conditions is expected. Obviously, for such situations, the results obtained in the previous subsections are modified. A prolonged stomatal closure under such situations must be limited in duration and frequency, otherwise, the vegetation would perish.

Case C4 (Fig. 7a) provides an example for a situation similar to Case C2 except for a relatively dry soil (a volumetric wetness of 5%) in the vegetated area. Retardation of the induced circulation characteristics as compared to Case C2 is evident by the reduction in the horizontal and vertical extent of the circulation, as well as the warmer PBL over the vegetated segment. Case C4* (Fig. 7b) is a repetition of Case C4, using the VER1 module. Simulation results in this case indicate, too, a circulation retardation, although not to the extent indicated in Case C4.

Additional insight into the impact of the soil wetness for intermediate soil wetness situations (between Case C2 and Case C4) was also considered. The results are presented in terms of the sensible heat fluxes (Fig. 8a). The daytime magnitude of the sensible heat flux in the middle of the vegetated segment is increased while the corresponding evapotranspiration is reduced significantly as the soil volumetric wetness below the canopy dropped from 25% to 5%. Based on the analytical evaluations provided in section 4 and the presented features of the sensible heat flux, it can be estimated how much the circulation will become weaker as the volumetric wetness below the canopy decreases.

Figure 8b illustrates the impact of an increase in the initial background atmospheric surface layer temperature on the sensible and latent heat fluxes from the vegetative segment in situations such as presented in Case C2. For an initial surface-layer temperature of 27°C (as in the original Case C2), the sensible heat fluxes are relatively low (with a peak value around 65 W m^{-2}). As the background surface-layer air temperature increases (to 32° and 37°C), the plant leaves enter stress conditions, resulting in partial closure of the stomata and consequently an increase in leaf temperature. Thus the sensible heat fluxes increase. The major importance that the stomata have in controlling the daytime sensible heat fluxes is illustrated by simulating a hypothetical stomatal opening ($d_s = 1$) for a surface-layer background initial temperature of 37°C. Transpiration involved under this relatively high temperature is very large and reduces sensible heat fluxes to negligible values.

Finally, an illustration of the influence of reduced atmospheric moisture in Case C2 on the thermal fluxes is given in Fig. 8c. According to the stomatal mechanism, a reduction in the atmospheric moisture and thus an increase of the VPD causes the plant to enter into stress conditions. For situations in which the specific humidity within the lower atmosphere was reduced initially from values given in Table 5 to 8 g kg^{-1} and 4 g kg^{-1}, a minor response of the stomata is indicated since the sensible heat fluxes are only slightly changed; however, as the lower atmosphere becomes even drier (2 g kg^{-1}), a pronounced increase in the sensible heat flux is simulated.

4) NONCONTINUOUS AND SPARSE VEGETATIVE COVER

When a fully developed vegetation canopy covers scattered portions of a grid area (i.e., covering only a fraction of the model grid area; $\sigma_f < 1$), the latent heat

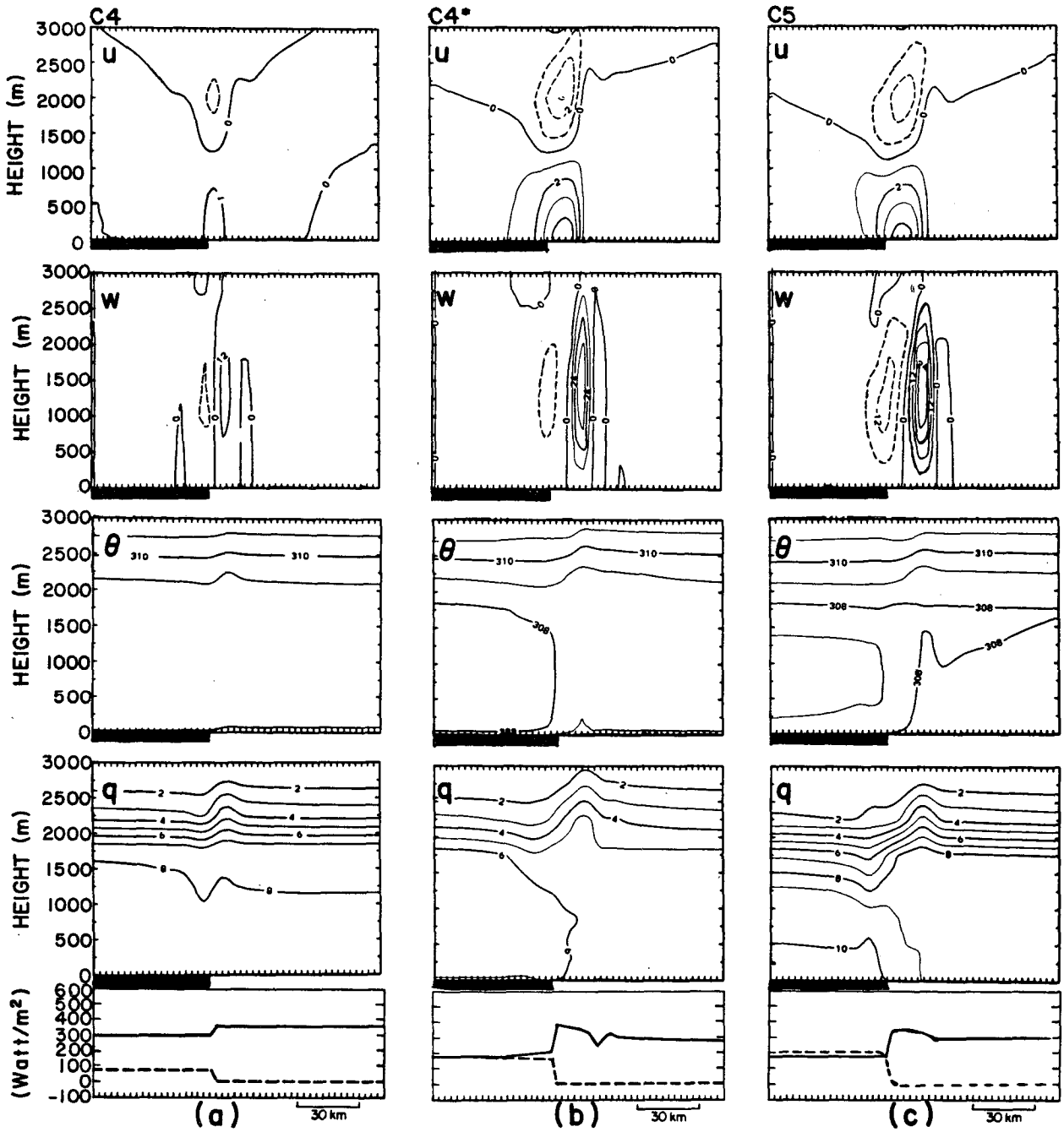

FIG. 7. As in Fig. 5, except for Cases C4, C4* and C5 (the dark segment indicates the vegetation section).

flux over these partially vegetated grid areas may increase somewhat due to subgrid advection effects. The contribution of latent heat flux by vegetation from the total grid area reduces, however, as compared to a fully vegetated grid, while the corresponding sensible heat flux increases. Consequently, the intensity of the thermally induced circulations between vegetated and adjacent bare dry soil areas is reduced. Figure 7c illustrates the simulation result obtained for Case C5 which is identical to Case C3 except for reducing the vegetation density to $\sigma_f = 0.25$ [while using the relation (16b)]. The pronounced retardation in the circulation is clearly evident. When a situation similar to Case C1 is considered, but with $0 < \sigma_f < 1$, and the soil surface remains wet, major differences in the simulated fields are not anticipated since the latent heat fluxes are likely to be only slightly changed. Thus, similar sensible heat fluxes in both cases are expected, but when that soil

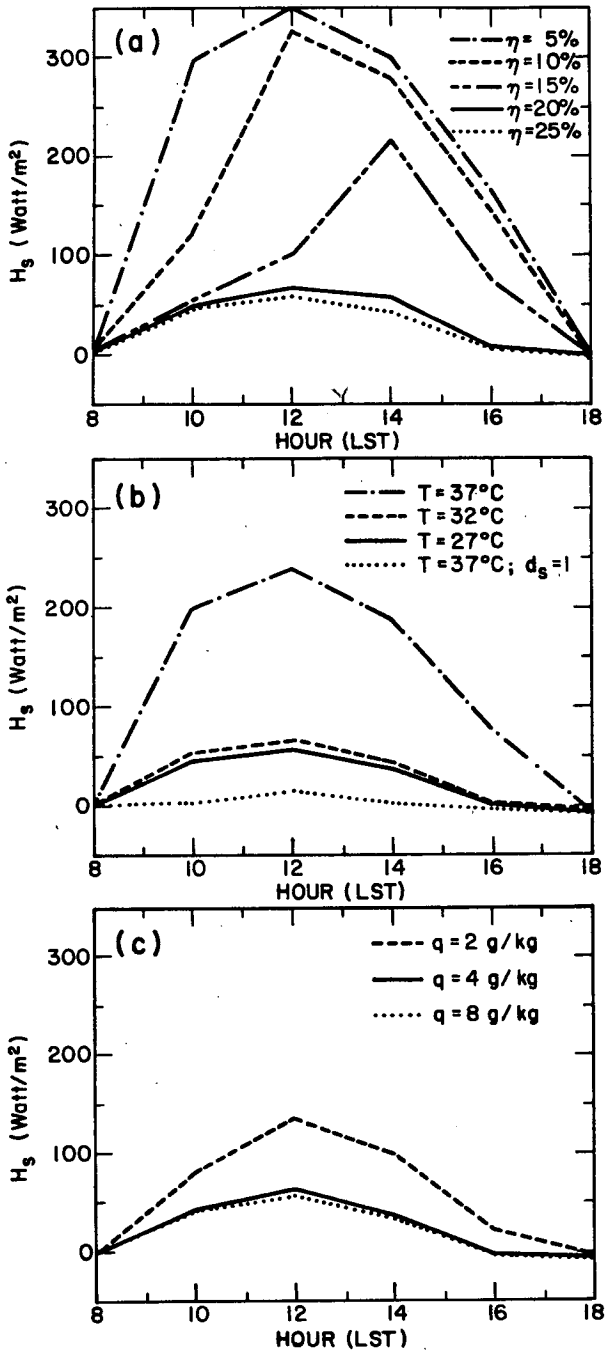

FIG. 8. (a) The variations of the sensible heat flux H_s with time in the middle of the vegetated section in simulations analogous to Case C1 however with soil volumetric wetness (η) values for the vegetated area as indicated; (b) The same as (a), however, with the initial surface-layer temperature as indicated; (c) The same as (a), however, with reductions of the atmospheric specific humidity to the stated values.

surface dries out and the subsoil layer within the root zone is still wet, a thermal circulation would be expected.

An illustration of the impact of vegetation cover density is provided in Fig. 9, where σ_f was reduced gradually from 1 to 0.25 for conditions similar to Case C2. Assuming row crops and thus using Eq. (16a), as σ_f reduces (due to increases in row spacing), the efficiency of transpiration from the canopy increases (as evident from the corresponding σ'_f values), although the total latent heat flux averaged over the grid area decreases. Physically as the canopy density is reduced, the sensible heat produced at the bare soil surface between the rows is advected over the canopy and is used to enhance transpiration which may then be larger than the available net radiation (e.g., Shaw and Decker 1977). Therefore, when the vegetative cover per unit area reduces, the effective transpiration/sensible heat flux from that unit area reduces/increases, however, nonlinearly. When similar σ^2 values were adopted in the model, however, assuming fractional coverage of the model grid by dense canopy (i.e., using Eq. 16b), the corresponding fluxes are modified somewhat. Additional model development is needed to accurately represent this case.

5) OASIS SIMULATIONS

On many occasions (mostly in semi-arid zones), the irrigated crop areas occur as an "island" within the arid surroundings (sometimes referred in the agrometeorological literature as an "oasis"). Case C6 presents simulation results involved with an oasis of 30 km width where the other surface characteristics are

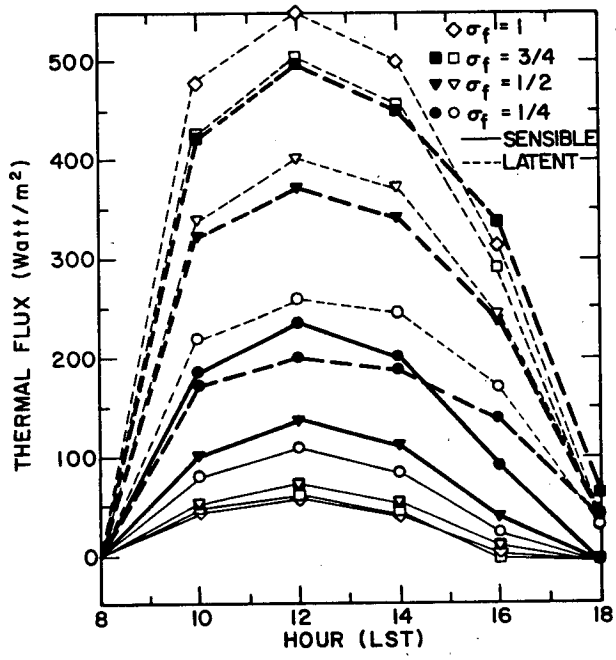

FIG. 9. As in Fig. 8a, however, with various σ_f values (thin lines indicates computations based on Eq. 16a; thick lines indicates computations based on Eq. 16b).

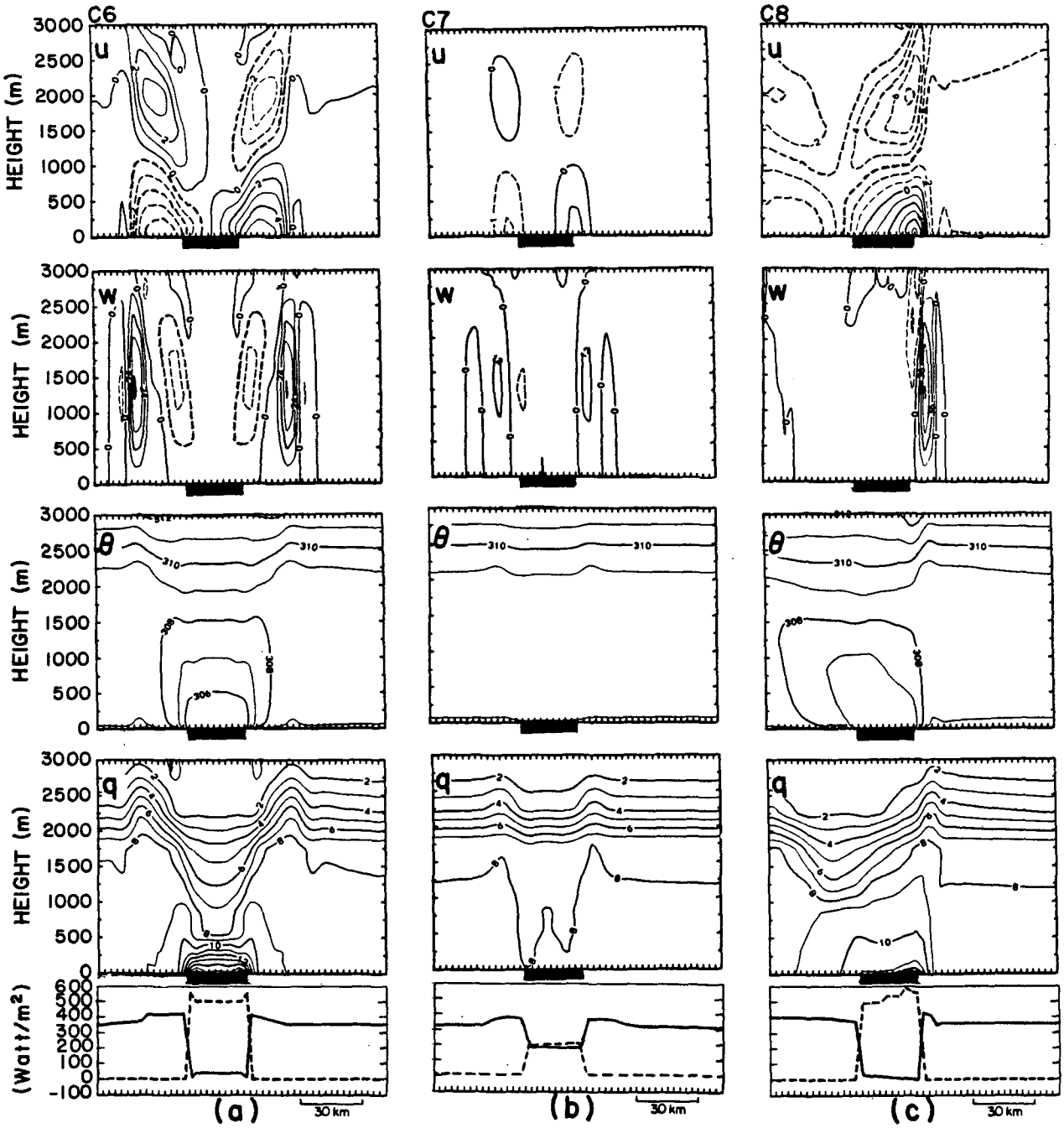

FIG. 10. As in Fig. 5, except for Cases C6, C7 and C8 (the dark segment indicates the vegetation section).

as in Case C2 (Fig. 10a). The anticipated two circulation cells, as well as the enhanced moistening in a shallow layer over the oasis, are pronounced. Between 500–1500 m, however, the air over the oasis is markedly drier than the surrounding. This is a response to the pair of thermally direct circulations, which enhance subsidence over the cooler surface of the oasis. For the same case but with $\sigma_f = 0.25$ (using the Eq. 16b), a significant retardation of the circulations is noticeable (Case C7; Fig. 10b). Repeating Case C6 however, with an easterly synoptic flow of 3 m s^{-1} considerably distorted the two cell circulation pattern while enhancing the convergence at the windward edge of the vegetated area (Case C8; Fig. 10c). Results obtained in the last case suggest that observational identification of the thermal circulation involved with an oasis becomes somewhat difficult when significant synoptic flow exists.

b. Flat terrain: influence of horizontal surface temperature gradient

Typically leaf life-supporting temperatures must be lower than ~55°C; however, in order to maintain its productive functioning, the leaf temperature should be lower than ~40°C (e.g., Larcher 1975). Observed leaf temperatures in well irrigated crops during the warm season are typically within the range of 30°–36°C in the subtropics and midlatitudes (e.g., Linacre 1964; Pau U 1984). When water stress conditions develop as the soil becomes dry, or when ambient environmental conditions are extreme, leaf temperatures may reach the threshold temperature for complete stomatal closure. In these situations the canopy surface temperature will not be maintained in the typical range of 30°–36°C and may increase considerably above that value.

Using this information regarding possible leaf temperatures, a model estimation of the magnitude of thermally induced circulations between a vegetated area and an adjacent bare soil region as a function of the horizontal gradient of surface temperature can be made. The simulations consider a sinusoidal change in time of the temperature contrast between a region of vegetation and an area of bare soil, with a peak temperature contrast, ΔT, at the local noon hour. This thermal contrast is established in two ways: (i) a step function change in the surface temperature reflecting a sharp transition from the vegetated to the bare soil section (see also analogous evaluations in Ookouchi et al. 1984); and (ii) a gradual linear change along some distance, reflecting a gradual reduction in vegetation density while moving towards the bare soil section. Illustrative circulation characteristics involved with such cases are provided in Table 7.

Case CT1 has a relatively mild contrast (growing sinusoidally from morning hours to a peak contrast value of ΔT = 5 K at noon), which is likely to occur when the canopy is under some thermal stress or when the adjacent bare soil is relatively wet. The relatively mild thermal contrast, as compared, for example, with the SBS case, results in comparatively insignificant circulation intensity characteristics (see Case SBS, Fig. 5a).

TABLE 7. The maximum near-surface u component ($u_{s_{max}}$) and the maximum u component and w within the simulated cross section (u_{max} and w_{max}, respectively) at 1400 LST. ΔT indicate the noon hour surface temperature difference across a distance L separating the cooler surface temperature portion of the domain from the warmer surface temperature portion of the domain.

$\Delta T/L$ (K/km)	$u_{s_{max}}$ (m s^{-1})	u_{max} (m s^{-1})	w_{max} (cm s^{-1})	Case
5/3	2.9	3.7	11	CT1
5/30	2.2	2.8	7	CT2
15/3	5.1	7.0	53	CT3
15/30	4.4	6.0	40	CT4
15/90	2.9	3.8	14	CT5

A step-function type of ΔT as assumed in Case CT1 is an idealized situation (i.e., a change from vegetation to a large bare soil area is not always sharply defined). In order to examine the circulation when ΔT is established gradually, the previous simulation was modified to consider temperature changes over a distance of 30 km (Case CT2). Surprisingly, even with the gradual change in surface temperature, the magnitude of the simulated u and w peak values were almost unaffected.

The peak values given in Table 7, for Cases CT3, CT4 and CT5, provide an example of the thermal circulation resulting from a relatively strong surface temperature contrast with ΔT = 15 K at the noon hour. Such an intensity contrast may be established, for example, between well irrigated crops and an adjacent dry bare soil area. Peak values of u and w, which are close in their magnitude to that of the sea breeze in Case SBS, (see Fig. 5a) are simulated to occur when the surface temperature change occurs over a distance of 3 km (CT3). When a gradual change of the surface temperature contrast along a distance of 30 km is considered (CT4), only relatively small differences are noticeable as compared to Case CT3. Even when that temperature change occurs across 90 km, a relatively weak circulation is noticeable (CT5).

Two examples of observed surface temperature contrasts between agricultural irrigated areas in juxtaposition to a grazed short-grass prairie region in Colorado are presented in Fig. 11. The examples provide the earth surface blackbody IR temperature derived from the GOES geostationary satellite (with a pixel resolution of 4 × 8 km) which were taken during the summer of 1986. Using the Denver radiosonde data, a correction for atmospheric water vapor absorption was included. Each image is a composite of the first 15 days of August at 1300 LST (when the surface temperature is around its daily peak value). Only areas with clear sky conditions, at that hour, were included in the construction of the composites. The vegetated areas (indicated by shading on the figures) were identified based on the Landsat image of Colorado for the end of June–beginning of July 1976 (available from the Earth Resources Department at CSU) as well as from the U.S. Department of Agriculture vegetation cover maps of Colorado.

The first example (Fig. 11a) is for northeast Colorado which includes the agricultural areas along the Front Range and the South Platte River. The topographical variations in the area presented are in the range of 200 m.

The second example is for the San Luis Valley (Fig. 11b) where there is intensive irrigated summer agricultural activity in the central domain. The valley is nearly flat, and it is surrounded by steep mountains to the southwest and northeast as indicated in the figure.

In both composites there is a significant correspondence between the cooler areas and vegetative cover. The highest temperatures occur in the uncultivated areas. Maximum IR surface-temperature gradients of

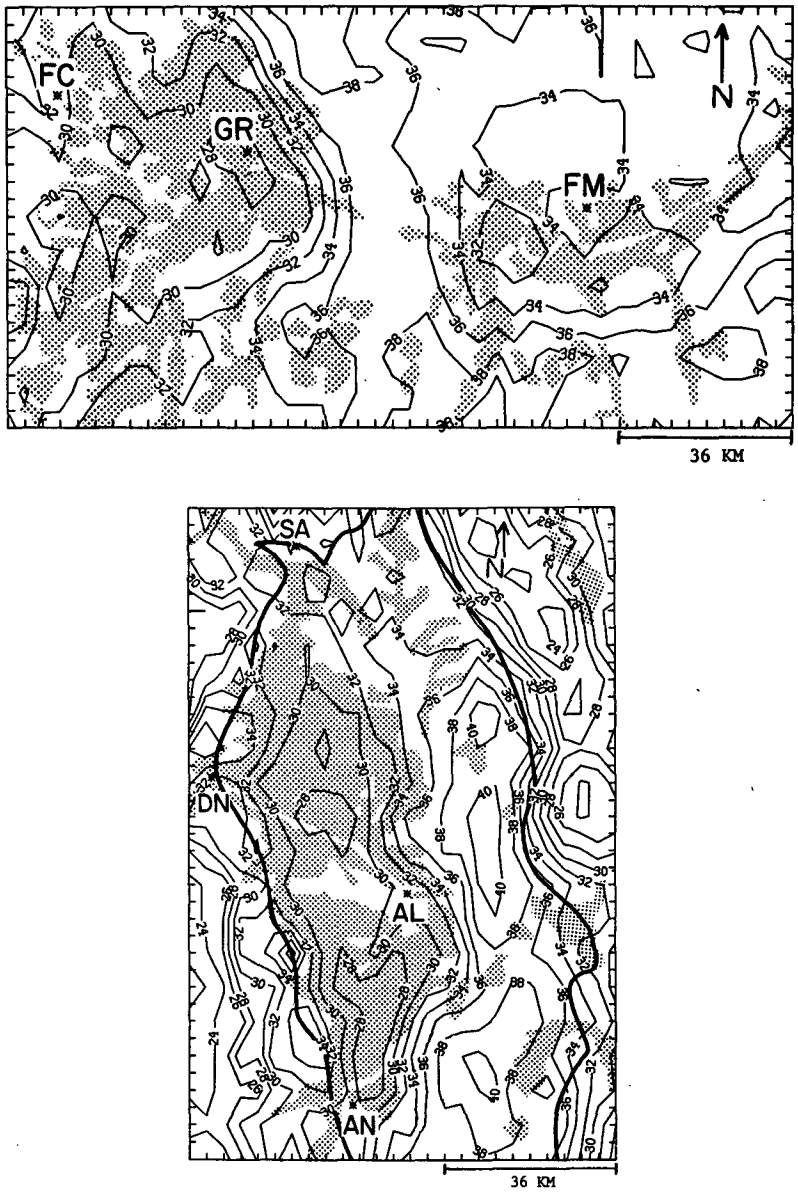

FIG. 11. Composite of GOES derived surface temperature at 1300 LST for the period 1 August 1986 to 15 August 1986 (a) for northeast Colorado (FC—Fort Collins; FM—Fort Morgan; GR—Greeley), (b) for the San Luis Valley in Colorado (AL—Alamosa; AN—Antonito; DN—Del Norte; SA—Saguache). The lower valley is outlined by a dark line separating it from significant elevated terrain. Irrigated areas are shaded.

10° and 12°C over distances of 10–20 km were observed in northeast Colorado and the San Luis Valley, respectively. Since the emittance of the earth surface is less than 1, the actual surface temperatures involved with these cases are somewhat higher than those presented. The emissivity of the irrigated area, however, is likely to be somewhat higher than that of its dryland surroundings (e.g., Lee 1978). Thus the actual surface-temperature gradients are suggested to be larger than those illustrated. Therefore, based on the simulations CT1–CT5 presented in this subsection, noticeable circulations should be expected to occur with such temperature gradients. The existence of thermally induced upslope flows in these specific locations are likely to mask their occurrence.

c. *Slope simulations*

A slope, with a horizontal extent of 30 km adjacent to a plateau at a height of 1000 m, was adopted to examine the influence of vegetation on daytime slope circulations. The three simulated cases are outlined in Table 8. The simulations consist of a dry bare soil control case to which vegetated cases are compared.

TABLE 8. Description of the simulated slope cases. Vegetation type 1 indicates trees; vegetation type 2 indicates crops.

Case	Volumetric soil wetness (%)	/Vegetation type/σ_f/LAI/	Figure
SL1	5	—	12a
SL2	25	/1/1/3/ all domain	12b
SL3	5	/1/1/3/ all domain	12c

With a dry slope (Case SL1), as illustrated in Fig. 12a, the u component reaches a peak value of 6 m s^{-1} by 1400 LST along the upper slope, while the circulation penetrates onto the plateau. The vertical velocities, associated with the edge of the penetrating flow over the plateau, reach a value of over 48 cm s^{-1}, which is significantly stronger than the velocities simulated over the slope itself. The PBL depth, as indicated by the θ field structure, is about 2000 m. This depth is nearly identical to the depth of the upslope flow. The similar depth of both layers supports the assumption made in the analytical evaluation presented in section 4 concerning such a relation. The moisture field is relatively low due to induced evaporation and the well developed PBL.

Case SL2 is the same as Case SL1 except that a relatively wet soil was prescribed and a vegetation cover is imposed. As shown in Fig. 12b the latent heat flux reaches values of ~500 W m^{-2}, and therefore considerably suppresses the sensible heat fluxes. As a result, a weak upslope circulation is generated as indicated by the upslope flow peak speed of only 3 m s^{-1}, and, thus, reduced vertical velocities over the plateau. Rather weak vertical velocities, with a peak of around 6 cm s^{-1}, are simulated along the slope. The suppression of the sensible heat fluxes results in a shallow PBL as evidenced by the θ field.

Case SL3 is similar to Case SL2 except for imposing stress conditions on the vegetation by reducing the initial soil volumetric wetness. As evident from Fig. 12c, the resulting characteristics of u, w, θ and q are about midway between Cases SL1 and SL2.

d. Scaling evaluation

Additional evaluation of the intensity of the circulations involved with the VER2 cases which were described in Tables 6 and 8 is provided in the present subsection. A comparison between the relations given in Eqs. 10 and 11 and the model simulation results is shown. (The observational data and evaluations of the impact of vegetative surfaces on sensible heat fluxes given in section 3 can be used for general scaling.) The magnitude of $\int_A^B u_s dl$ is used as an indicator of the intensity of the surface induced flow and its horizontal extent. The analytical expressions for the surface line circulation given in Eqs. 10 and 11 were evaluated using t = 21 000 s, while adopting a sinusoidal variation of H_s with time which acquires a peak value at noon as indicated in Table 9. The numerical model estimation of the surface line circulation is given for 1400 LST (6 hours following the commencement of the simulation).

Estimation of α values is obtained using the approximation

$$\frac{\partial \overline{u'w'}}{\partial z} = \frac{C_D u_s^2}{h_D} = \alpha u_s \tag{20}$$

where C_D is the surface drag coefficient and h_D is the depth within which the u component of momentum flux, ($\overline{u'w'}$), reduces to 0, i.e., the level of the wind maximum or the top of the PBL. The value of C_D can be approximated as:

$$C_D = \left[\frac{k_0}{ln(z(1)/z_0)}\right]^2 \tag{21}$$

where k_0 = 0.35 is the von Kármán constant; and $z(1)$ is the first model level height (5 m). Usually h_D is the height of the PBL, but when a wind maximum exists within the PBL, h_D is defined as the height of the wind speed maximum. It should be stated, however, that in a weakly convective PBL, momentum transfer through the wind maximum layer is likely to occur due to surface generated buoyancy. In a strongly mixed convective PBL no wind maximum would exist and h_D would be equated with the PBL top. In the model simulations in this study a weak wind maximum exists with a typical simulated noon hour peak wind at h_D = 40–100 m (as can be roughly estimated from the presented simulated wind fields). The corresponding u_s values were in the range of 1–5 m s^{-1}. Using Eqs. (20) and (21) and the surface roughness parameters which were used in the simulations, the values of α were approximated. Finally, it should be noted that as the day proceeds the values of u_s and h_D increase, suggesting that the α values derived using Eq. (20) does not vary rapidly.

It is suggested that Eq. (10) would overestimate the circulation since in the real world advection would reduce the horizontal temperature gradient associated with the right-hand side of Eq. (10). This potential overestimation is likely to be most pronounced when the sensible heat fluxes difference, $H_{s_1} - H_{s_2}$, in Eq. (10) is extremely small. For the slope cases, the extension of the circulation toward the plateau and somewhat to the lower plain reduces the flow intensity along the slope as compared to the ideal infinite long slope assumed in the derivation of Eq. (11). In order to compensate for the overestimations involved with the derivation of the surface line circulations while using Eqs. (10) and (11) an effective adjustment of α (i.e., increase of α values), which extends the original meaning of α introduced in section 4, is required.

It was found that, while using Eq. (10) (for relatively large values of $H_{s_1} - H_{s_2}$), the estimated values of α through Eqs. (20)–(21) should be doubled for an appropriate agreement of the scaled circulation while

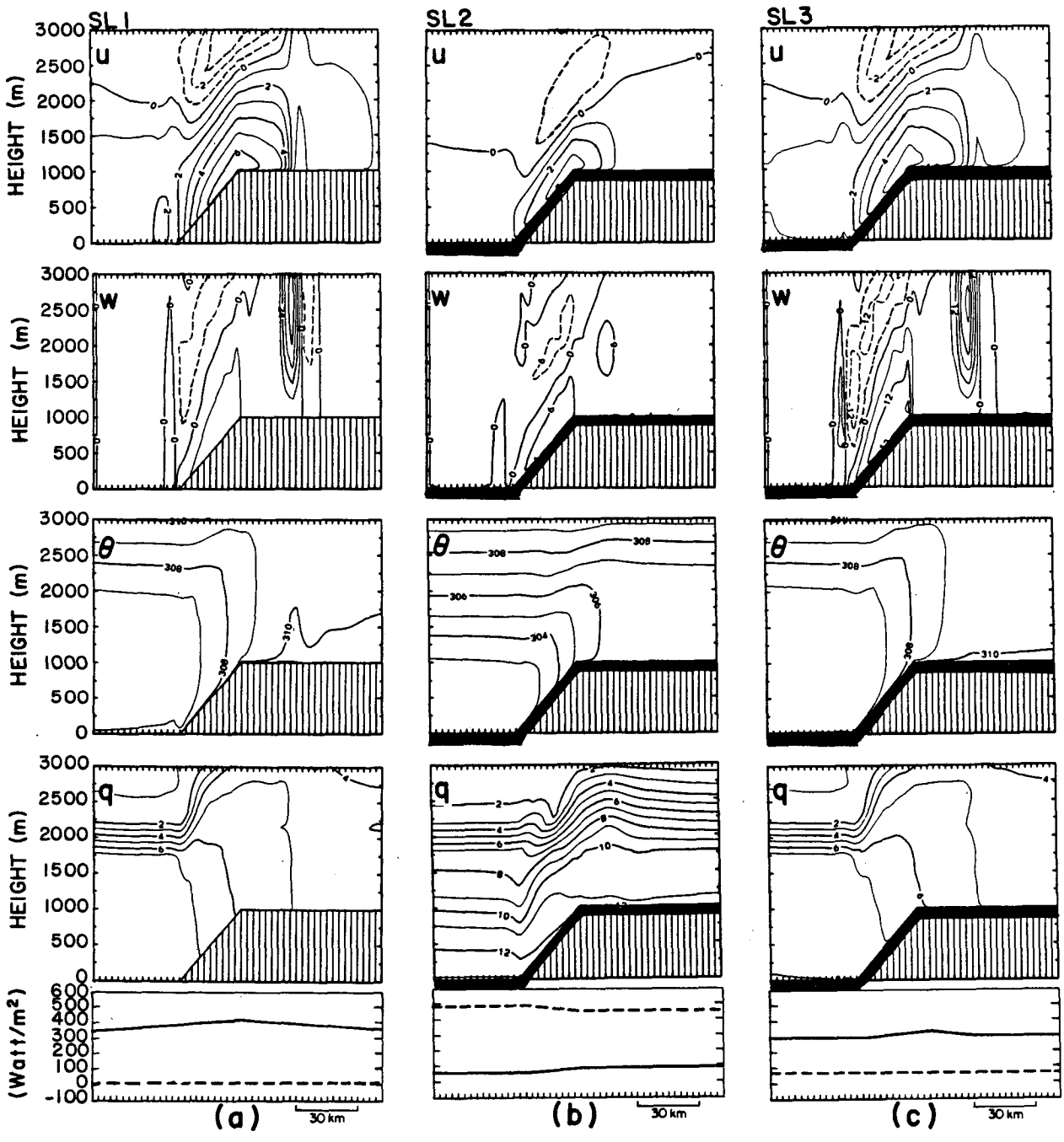

FIG. 12. As in Fig. 4, except for Cases SL1, SL2, and SL3 (see Table 7 for their definition). The dark segment indicates the vegetation section.

compared with that obtained from the numerical model results. For small values of $H_{s_1} - H_{s_2}$, however, (in this study indicated to be below ~ 50 W m^{-2}) a more significant increase in the values of α is required for such a purpose. The last situations are therefore not considered for the scaling. When the slope cases (SL1–SL3) were considered it was also found that for these cases the α values have to be doubled in order to fit the numerical model results. The values of α used for the scaling purpose as outlined above are provided in Table 9.

7. Conclusion and discussion

The present study evaluates the possible impact of vegetative areas on typical daytime thermally induced mesoscale circulations (i.e., sea breeze and upslope flows) as well as the generation of mesoscale circula-

TABLE 9. Evaluation of the magnitude of $\int_A^B u_s dl$ 6 hours following the commencement of the thermal circulation (1400 LST).

Case	H_s		α	$\int_A^B u_s dl$	
	Vegetation (sea)	Bare soil (W m^{-2})	(s^{-1})	Model ($m^2 s^{-1}$)	Based on Eqs. (10)–(11) ($m^2 s^{-1}$)
SBS	~0	375	0.30×10^{-3}	3.15×10^5	3.54×10^5
SBV	~0	50	0.21×10^{-3}	4.28×10^4	4.98×10^4
C1	49	62	0.35×10^{-3}	4.17×10^3	—
C2	37	400	0.43×10^{-3}	2.22×10^5	2.60×10^5
C3	30	400	0.43×10^{-3}	2.26×10^5	2.57×10^5
C4	302	353	0.18×10^{-3}	1.31×10^4	6.50×10^4
C5	170	350	0.40×10^{-3}	7.37×10^4	1.02×10^5
SL1	—	395	0.8×10^{-3}	1.33×10^5	1.41×10^5
SL2	80	—	1.3×10^{-3}	3.60×10^4	4.45×10^4
SL3	330	—	1.7×10^{-3}	6.00×10^4	6.98×10^4

tions due to nonuniform vegetation cover. The characteristics of vegetation and the immediate environment associated with the modification of evapotranspiration, and consequently of the sensible heat fluxes, were evaluated. Observational data of evapotranspiration rates were given in order to support a scale analysis involved with those circulations. Numerical model simulations provided a quantitative evaluation for several selected situations. A negligible synoptic flow was assumed in most of the simulations presented in this study in order to provide basic evaluations of the involved circulations. Obviously, the existence of synoptic flow or other background flow would modify the simulated circulation features, where such strong flows would mask the existence of these circulations. As suggested in Ookouchi et al. (1984), such impacts can be projected based on available documentation of sea breeze and mountain thermally induced circulation coupling with background flows. Much more study of the influence of vegetation on mesoscale circulations needs to be performed in order to obtain a refined insight into its effect. Such study should emphasize observations and classification of geographical locations with vegetation where relatively substantial mesoscale impacts should be expected. Mostly, it should evaluate if the pronounced circulations developed under the prescribed ideal situations assumed in the present study are also a real world feature.

Several general conclusions can be made based on the present study:

(i) Mesoscale domains covered over an extended portion by very dense vegetation that is not under water or environmental stress, when adjacent to bare soil area, can generate a thermal circulation comparable in intensity to a sea breeze. On the other hand, suppression of daytime upslope flows due to very dense vegetation coverage of the slope is pronounced, at least for the vegetation types, and soil wetness characteristics applied in this study.

(ii) Reductions in the density of vegetation coverage of a local area (i.e., wide gaps of bare soil), which is typical of most real world situations, reduce the impact obtained with the ideal uniform vegetation coverage described in (i). In addition, water and thermal stresses resulting from ambient environmental conditions which should be considered in the real world situations reduce the evapotranspiration rates, and increase the effective sensible heat fluxes from the vegetative cover.

(iii) Following a continuous drought, but with water available to the roots of vegetation, a major difference in evapotranspiration features is established between a vegetated and a bare soil area. In the vegetated area, root extraction of moisture from the deep wet soil layers enables effective transpiration while in the bare soil area evaporation is effectively eliminated. This situation may result in well-defined thermally forced circulations.

(iv) It was shown that there is no substantial difference in the thermally forced mesoscale circulation generated by a sharp thermal contrast along flat terrain (i.e., as resulting from a well defined vegetated area in juxtaposition to bare soil), when compared to that generated by an equivalent, although somewhat gradual change, in the thermal contrast (i.e., as resulting from a gradual change from dense vegetated area to a bare soil surrounding). In the specific simulations presented in the present study, this conclusion is valid for a gradual change along distances $\leq$30 km.

(v) Vegetated areas over wet soil, and bare wet soil areas, are of closely equivalent forcing in generating the circulations evaluated in the present study.

(vi) GOES IR images of surface temperature over two locations in Colorado show substantial contrasts of surface temperature generated during the summer between irrigated crop areas adjacent mostly to dry land regions (similar IR surface temperature features were found when the study was extended to other large irrigated areas in the western United States).

(vii) The study provided observational and modeling evaluations relevant to the impact of vegetative cover on mesoscale thermal circulations. The task of incorporating accurate vegetation characteristics and pertinent environmental conditions into numerical

model simulations for specific cases is crucial in order to obtain adequate estimations of their impact. As implied from this study, the incorrect specification of these characteristics will lead to significant simulation errors. The advancement in satellite imagery resolution provides an excellent perspective for a reasonable definition of vegetative surfaces as well as several physical characteristics of vegetated and bare soil areas needed for model simulations (e.g., Tucker et al. 1984; McGinnis and Tarpley 1985; Wetzel and Woodward 1987).

Acknowledgments. Part of this study was carried out in the Fall 1985 while the senior author visited the Seagram Centre for Soil and Water Sciences, at the University of Jerusalem. He would like to thank Y. Mahrer, O. Naot and E. Ravitz for useful discussions during that visit. R. Dickinson, H. Duke, J. R. Garratt, L. Mahrt, M. Mandel and J. Sheaffer provided useful comments on the manuscript. The authors wish to thank J. Weaver, A. Lipton, A. Jones, and J. Purdom for their help with the collection, processing and the interpretation of the satellite IR images. The study was supported by the NSF under Grants ATM-8414181 and ATM8616662, by EPRI under Contract RP-1630-53, by NASA under grant NAG-5359, and by NOAA under grant NA85RAH05045. The computations were carried out by the NCAR CRAY Computer (NCAR is supported by the NSF). The manuscript was prepared by Sandra Wittler and Linda Jensen.

REFERENCES

Aase, J. K., and F. H. Siddoway, 1982: Evaporative flux from wheat and fallow in semiarid climate. *Soil Sci. Amer. J.*, **46,** 619–626.

Abbs, D. J., and R. A. Pielke, 1986: Thermally forced surface flow and convergence patterns over northeast Colorado. *Mon. Wea. Rev.*, **114,** 2281–2296.

Alpert, P., and M. Mandel, 1986: Wind variability—an indicator for a meso-climate change in Israel. *J. Climate Appl. Meteor.*, **25,** 1568–1567.

Anthes, R. A., 1978: The height of the planetary boundary layer and the production of circulation in a sea breeze model. *J. Atmos. Sci.*, **35,** 1231–1239.

——, 1984: Enhancement of convective precipitation by mesoscale variations in vegetative covering in semiarid regions. *J. Clim. Appl. Meteor.*, **23,** 541–554.

Avissar, R., and Y. Mahrer, 1982: Verification study of a numerical greenhouse microclimate model. *Trans. Amer. Soc. Agric. Eng.*, **25,** 1711–1720.

——, and ——, 1986: Water desalination in solar earth stills: A numerical study. *Water Resour. Res.*, **22,** 1067–1075.

——, and ——, 1988: Mapping frost-sensitive areas with a three-dimensional local scale numerical model. Part I: Physical and numerical aspects. *J. Climate Appl. Meteor.*, **27,** 400–413.

——, P. Avissar, Y. Mahrer and B. A. Bravdo, 1985: A model to simulate response of plant stomata to environmental conditions. *Agric. For. Meteorol.*, **34,** 21–29.

——, N. Dagan and Y. Mahrer, 1986: Evaluation, in real time, of the actual evapotranspiration using a numerical model. Agrotique 86, Automation and robots for Agriculture, Bordeaux, France, 255–263.

Barnston, A. G., and P. T. Schikedanz, 1984: The effect of irrigation on warm season precipitation in the southern great plains. *J. Climate Appl. Meteor.*, **23,** 865–888.

Black, T. A., 1979: Evapotranspiration from Douglas fir stands exposed to soil water deficits. *Water Resour. Res.*, **15,** 164–170.

Brutsaert, W., 1982: Vertical flux of moisture and heat at bare soil surface. *In:* Land Surface Processes in Atmospheric General Circulation Models, P. S. Eagleson, Ed., Cambridge University Press, 115–168.

Budyko, M. I., 1977: *Climatic Change,* Amer. Geophys. Union, Waverly Press, 261 pp.

Burman, R. D., J. L. Wright and M. E. Jensen, 1975: Changes in climate and estimated evaporation across a large irrigated area in Idaho. *Trans. ASAE,* **18,** 1089–1093.

——, —— and J. D. Marwitz, 1977: Climate modification of dry desert air by a large irrigation project, 6th Conference on Planned and Inadvertent Weather Modification, Amer. Meteor. Soc., Champaign-Urbana, 81–82.

Businger, J. A., J. C. Wyngaard, Y. Izumi and E. F. Bradley, 1971: Flux profile relationship in the atmospheric surface layer. *J. Atmos. Sci.*, **28,** 181–189.

Clapp, R., and G. Hornberger, 1978: Empirical equations for some soil hydraulic properties. *Water Resour. Res.*, **14,** 601–604.

Danielson, R. E., 1967: Root systems in relation to irrigation. *Irrigation of Agricultural Land,* R. M. Hagen, M. R. Haise and T. W. Edminster, Eds., Amer. Soc. of Agronomy, Madison, Wisconsin, 390–424.

Davenport, D. C., and J. P. Hudson, 1967: Meteorological observations and Penman estimates along a 17 km transect in the Sudan Gezira. *Agric. Meteor.*, **4,** 405–414.

Davis, J. A., and S. B. Idso, 1979: Estimating the surface radiation balance and its components. *Modification of the Aerial Environment of Crops.* T. B. Barfield and J. F. Greber, Eds., Amer. Soc. of Agric. Eng. 183–210, [ISN 79-50967].

Deardorff, J. W., 1978: Efficient prediction of ground surface temperature and moisture, with inclusion of layer of vegetation. *J. Geophys. Res.*, **83**(4), 1889–1903.

De Vries, D. A., 1963: Thermal properties of soils. *Physics of Plant Environment,* W. R. Van Wijk, Ed., North Holland, 210–235.

——, and J. W. Birch, 1961: The modification of climate near the ground by irrigation for pastures on the Riverine Plain. *Aust. J. Agric. Res.*, **12,** 260–272.

Duffie, J., and W. Beckman, 1974: *Solar Energy Thermal Processes.* Wiley, 762 pp.

Dzerdzeevskii, B. L., 1963: Meteorological parameters of the surface air layer over humid and dry sectors of the Trans-Volga Steppe. *Sukhoveis and Drought Control,* B. L. Dzerdzeevskii, Ed., Israel Program for Scientific Translations, Jerusalem, 162–180.

Fritchsen, L. J., 1982: The vertical fluxes of heat and moisture at a vegetated land surface. *Land Surface Processes in Atmospheric General Circulation Models,* P. S. Eagleson, Ed., Cambridge University Press, 169–226.

Garrett, A. J., 1982: A parameter study of interactions between convective clouds, the convective boundary layer, and forested surface. *Mon. Wea. Rev.*, **110,** 1041–1059.

Hammer, R. M., 1970: Cloud development and distribution around Khartoum. *Weather,* **25,** 411–414.

Hillel, D., 1982: *Introduction to Soil Physics,* Academic Press, 364 pp.

Holmes, R. M., 1970: Meso-scale effects of agriculture and a large prairie lake on the atmospheric boundary layer. *Agron. J.*, **62,** 546–549.

Jarvis, P. G., G. B. James and J. J. Landsberg, 1976: Coniferous forest. In: *Vegetation and the Atmosphere,* J. L. Monteith, Ed., Academic Press, 171–240.

——, and J. I. L. Morison, 1981: The control of transpiration and photosynthesis by stomata. In: *Stomatal Physiology,* 248–279, Society for Experimental Biology, University of Cambridge, [ISBN 0-521-23683-5].

Jensen, M. E., Ed., 1973: *Consumptive Use of Water and Irrigation Water Requirements,* Amer. Soc. of Civil Eng. 215 pp.

Kaufmann, M. R., 1984: A canopy model (RM-CWU) for determining transpiration of subalpine forests. I. Model development. *Can. J. Fores. Res.*, **14,** 218–226.

Larcher, W. L., 1975: *Physiological Plant Ecology,* Springer-Verlag, 252 pp.

Lee, R., 1978: *Forest Micrometeorology,* Columbia University Press, 276 pp.

Linacre, E. T., 1964: A note of feature of leaf and air temperatures. *Agric. Meteor.*, **1,** 66–72.

Lomas, J., and M. Mandel, 1973: The quantitative effects of two methods of sprinkler irrigation on the microclimate of mature avocado plantation. *Agric. Meteor.*, **12,** 35–48.

Mahrer, Y., and R. Avissar, 1985: A numerical study of the effects of soil surface shape upon the temperature and moisture profiles. *Soil Sci.*, **139,** 483–490.

——, and R. A. Pielke, 1977: A numerical study of air flow over irregular terrain. *Contrib. Atmos. Phys.*, **50,** 98–113.

——, O. Naot, E. Rawitz and Y. Katan, 1984: Temperature and moisture regimes in soils mulched with transparent polyethylene. *Soil Sci. Soc. Amer. J.*, **48,** 362–367.

Martin, C. L., D. Fitzjarrald, M. Garstang, A. P. Oliveira, S. Greco and E. Browell, 1988: Structure and growth of the mixing layer over the Amazonian rain forest. *J. Geophys. Res.*, **93**(D2), 1361–1375.

McCumber, M. C., 1980: A numerical simulation of the influence of heat and moisture fluxes upon mesoscale circulations. Ph.D. dissertation, Department of Environmental Science, University of Virginia, Charlottesville, 255 pp.

——, and R. A. Pielke, 1981: Simulation of the effects of surface fluxes of heat and moisture in mesoscale numerical model. Part I: Soil layer. *J. Geophys. Res.*, **86,** 9929–9938.

McGinnis, D. F., and J. D. Tarpley, 1985: Vegetation cover mapping from NOAA/AVHRR. *Adv. Space Res.*, **5,** 359–369.

McNider, R. T., and R. A. Pielke, 1981: Diurnal boundary-layer development over sloping terrain. *J. Atmos. Sci.*, **38,** 2198–2212.

Molz, E., and I. Remson, 1970: Extraction of term models of soil moisture use by transpiring plants. *Water Resour. Res.*, **6,** 1346–1356.

Monteith, J. L., Ed., 1976: *Vegetation and the Atmosphere, Vol. 2,* Academic Press, 439 pp.

Ookouchi, Y., M. Segal, R. C. Kessler and R. A. Pielke, 1984: Evaluation of soil moisture effects on generation and modification of mesoscale circulations. *Mon. Wea. Rev.*, **11,** 2281–2292.

Pan, H.-L., and L. Mahrt, 1987: Interaction between soil hydrology and boundary-layer development. *Bound. Layer Meteor.*, **38,** 185–202.

Pau U, K. T., 1984: A theoretical basis for the leaf equivalence point temperature. *Agric. Meteor.*, **30,** 247–256.

Philip, J. R., and D. A. De Vries, 1957: Moisture movement in porous materials under temperature gradients. *Trans. Amer. Geophys. Union,* **38,** 222–232.

Pielke, R. A., 1974: A three-dimensional numerical model of the sea breezes over south Florida. *Mon. Wea. Rev.*, **102,** 115–139.

——, and Y. Mahrer, 1975: Technique to represent the heated-planetary boundary layer in mesoscale models with coarse vertical resolution. *J. Atmos. Sci.*, **32,** 2288–2308.

——, and ——, 1978: Verification analysis of the University of Virginia three-dimensional mesoscale model prediction over south Florida for July 1, 1973. *Mon. Wea. Rev.*, **106,** 1568–1589.

——, and M. Segal, 1986: Mesoscale circulations forced by differential heating. In: *Mesoscale Meteorology and Forecasting,* Ray, P., Ed., American Meteorology Society, 516–548.

Reddy, S. J., 1983: A simple method of estimating the soil water balance. *Agric. Meteor.*, **28,** 1–17.

Ritchie, J. T., 1971: Dryland evaporative flux in a subhumid climate: I. Micrometeorological influences. *Agron. J.*, **63,** 51–55.

——, and F. Burnett, 1971: Dryland evaporative flux in a subhumid climate: II. Plant influences. *Agron. J.*, **63,** 56–62.

Rogerson, T. L., 1976: Soil water deficits under forested and clearest areas in northern Arkansas. *Soil Sci. Soc. Amer. J.*, **40,** 802–805.

Rutter, A. J., 1968: Water consumption by forests. In *Water Deficits and Plant Growth,* II. T. T. Kozlowski, Ed., Academic Press, 23–84.

——, 1975: The hydrological cycle in vegetation. In *Vegetation and the Atmosphere Vol. 1,* J. L. Monteith, Ed., Academic Press, 111–150.

Schneider, S. R., D. F. McGinnis, and G. Stephens, 1985: Monitoring Africa's Lake Chad basin with LANDSAT and NOAA satellite data. *Int. J. Remote Sens.*, **6,** 59–73.

Sebba, R., R. Enis and M. E. Hoffman, 1984: The Kibbutz landscape in arid zones. *Energy Building,* **7,** 205–211.

Segal, M., Y. Mahrer and R. A. Pielke, 1982: Application of a numerical mesoscale model for the evaluation of seasonal persistent regional climatological patterns. *J. App. Meteor.*, **21,** 1754–1762.

——, R. A. Pielke and Y. Mahrer, 1984: Evaluation of surface sensible heat flux effects on generation and modification at mesoscale circulations. Proceedings of the Second International Symposium on Nowcasting, European Space Agency, Norrkoping, Sweden, 263–269.

——, J. F. W. Purdom, J. L. Song, R. A. Pielke and Y. Mahrer, 1986: Evaluation of cloud shading effects on the generation and modification of mesoscale circulations. *Mon. Wea. Rev.*, **114,** 1201–1212.

Sellers, P. J., Y. Mintz, Y. C. Sud and A. Dalcher, 1986: A simple biosphere model (SiB) for use within general circulation models. *J. Atmos. Sci.*, **43,** 505–531.

Shaw, R. H., and W. L. Decker, 1977: The general heat balance of canopies. *Modification of the Aerial Environment of Plants,* B. J. Barfield and J. F. Gerber, Eds., American Society of Agricultural Engineers, 141–155.

Szeicz, G., C. H. M. Van Bavel and S. Takami, 1973: Stomatal factor in water use and dry matter production by sorghum. *Agr. Meteor.*, **12,** 361–389.

Tanner, C. B., 1960: Energy balance approach to evapotranspiration from crops. *Soil Sci. Soc. Amer. Proc.*, **24,** 1–9.

Tennekes, H., 1973: A model for the dynamics of the inversion above a convective boundary layer. *J. Atmos. Sci.*, **30,** 558–567.

Tucker, C. J., J. A. Gatlin and S. R. Schneider, 1984: Monitoring vegetation in the Nile Delta with NOAA-6 and NOAA-7 AVHRR imagery. *Photog. Engin. Remote Sens.*, **50,** 53–61.

Voronstov, P. A., 1963: Local air circulations in regions with ameliorated climate. *Sukhoveis and Drought Control,* B. L. Dzerdzeevskii, Ed., Israel Program for Scientific Translations, Jerusalem, 287–294.

Wetzel, P. J., and R. H. Woodward, 1987: Soil moisture estimation using GOES-VISSR infrared data: A case study with a simple statistical method. *J. Climate Appl. Meteor.*, **26,** 18–27.

Wilson, J. W., and W. E. Schreiber, 1986: Initiation of cloud convective storms at radar observed boundary-layer convergence lines. *Mon. Wea. Rev.*, **114,** 2516–2536.

Wyllie, M. R. J., and G. H. F. Gardner, 1958: The generalized Kozeney-Carman equation. *World Oil,* **146,** 210–228.

Yamada, T., 1982: A numerical model simulation of turbulent airflow in and above canopy. *J. Meteor. Soc. Japan,* **60,** 439–454.